

**Link sito dell'editore:**

<https://www.sciencedirect.com/science/article/abs/pii/S1359431117319555?via%3Dihub>

**Link codice DOI:** <https://doi.org/10.1016/j.applthermaleng.2017.08.042>

**Citazione bibliografica dell'articolo: G. Colangelo, E. Favale, M. Milanese, A. de Risi, D. Laforgia,  
Cooling of electronic devices: Nanofluids contribution,  
Applied Thermal Engineering,  
Volume 127,  
2017,  
Pages 421-435,  
ISSN 1359-4311,**

# COOLING OF ELECTRONIC DEVICES: NANOFLUIDS CONTRIBUTION

Colangelo G.\*, Favale E., Milanese M., de Risi A., Laforgia D.

Department of Engineering of Innovation – University of Salento  
Via per Arnesano – Lecce – Italy

## Abstract

Cooling of electronic devices is one of the main challenge of new generation technology. The extreme miniaturization has high benefits, but the heat to be dissipated per unit of surface increases in uncontrolled way. In this paper the application of a new generation of heat transfer fluids, nanofluids, to electronic devices is analyzed. Even if the use of nanofluids is not still common, there are many papers that deal with this topic, reporting both experimental and theoretical results. The development of this technology could be one of the key elements that could give an important impulse to further miniaturization of electronic devices and at the same time increase their energy efficiency.

**Keywords:** nanofluid, heat transfer, cooling, electronics.

## 1. Introduction

In the last two decades, many efforts have been made to enhance thermal properties of heat transfer fluids, as thermal conductivity. Particular attention has been given to liquid/solid suspensions, made with traditional heat transfer fluids and nanoparticles (<100 nm) of metal or metal oxide, that Choi [1] was the first to call nanofluids. Generally, the addition of nanoparticles yields an enhancement of thermal conductivity that depends on volume fraction of solid phase, particle size, material etc., as demonstrated by several authors. Colangelo *et al.* [2] showed the experimental results on diathermic oil based nanofluids, demonstrating better performance with respect to water based nanofluids with the same nanoparticles. Xie *et al.* [3] carried out a comparison between experiments and theoretical models, showing that the measured thermal conductivity in nanofluids is much higher than the values calculated using theoretical correlation, indicating new heat transport mechanisms. Xue [4] obtained an increase of 20.0% for 4.0%vol of CuO nanoparticles with an average diameter of 35 nm dispersed in ethylene glycol. Li *et al.* [5] found that thermal conductivity of Al<sub>2</sub>O<sub>3</sub>-water nanofluid at 6.0%vol was 1.52 times higher than water. Minsta *et al.* [6] measured thermal conductivity of CuO-water and Al<sub>2</sub>O<sub>3</sub>-water nanofluids. They obtained an increase between 2.0% and 24.0% at room temperature, for a volume fraction between 1.0% and 14.0% of CuO. Analogously, enhancements up to 30.0% with Al<sub>2</sub>O<sub>3</sub>-water at a volume fraction between 1.0% and 18.0% have been measured. Yu *et al.* [7] measured thermal conductivity of ZnO-ethylene glycol nanofluid. At 5.0%vol of solid phase, thermal conductivity was 26.5% higher than water.

Furthermore, several articles report too high values of thermal conductivity enhancement, not consistent with the remaining literature. For instance, by using Cu nanoparticles, with an average diameter lesser than 10 nm and ethylene glycol, Eastman *et al.* [8] obtained an increase of thermal conductivity of 40.0% at 0.3%vol of solid phase.

Nanofluids enhance also convective heat transfer coefficient, as Wen *et al.* [9] demonstrated with Al<sub>2</sub>O<sub>3</sub>-water nanofluid, flowing in a copper pipe with diameter of 4.5 mm, in laminar conditions: enhancement up to 47.0% at the entrance region has been obtained with a volume fraction of 1.6%. Rashidi *et al.* [10] tested Multiwall Carbon Nanotubes (MWCNT)-water nanofluid at weight fraction of 2.0% in a copper tube with inner diameter of 6.0 mm obtaining convective heat transfer coefficient as a function of the axial distance from inlet. A convective heat transfer coefficient enhancement up to 8.0% with Al<sub>2</sub>O<sub>3</sub>-water nanofluid at 0.3%vol has been measured in a stainless tube by Hwang *et al.* [11]. Al<sub>2</sub>O<sub>3</sub>-water nanofluid in a stainless tube with an inner diameter of 4.57 mm has been studied by Kim *et al.* [12]. They obtained an increase of heat transfer coefficient of

15.0% and 20.0% under laminar and turbulent flow conditions respectively. Colangelo *et al.* [13] experimentally investigated Al<sub>2</sub>O<sub>3</sub>-water nanofluid in an aluminum tube with inner diameter of 15.0 mm. With a volume fraction of 3.0%, enhancement of 25.0% compared with water was obtained. Heyhat *et al.* [14] investigated on convective heat transfer coefficient in a circular tube at constant wall temperature with Al<sub>2</sub>O<sub>3</sub>-water nanofluid with a volume fraction from 0.1% to 2.0%. Enhancements up to 23.0% have been obtained in comparison with water.

The increase of thermal conductivity and convective heat transfer coefficient have prompted the researchers to study stability of nanofluids, as Colangelo *et al.* [15], and their effects on engines cooling and energy production systems. Tzeng *et al.* [16] experimentally investigated the effects of CuO and Al<sub>2</sub>O<sub>3</sub> on engine transmission oil at 4 engine operation speeds. The lowest temperature has been obtained with CuO nanoparticles. Bai *et al.* [17] numerically analyzed an engine cooling system with nanofluid as heat transfer fluid. Good results have been obtained with Cu-water nanofluid: with a concentration of 5.0% heat dissipating capability increased by 44.1%. Marè *et al.* [18] obtained an increase of heat transfer coefficient of 42.0% and 50.0% with Al<sub>2</sub>O<sub>3</sub>-water nanofluid and Carbon Nanotubes (CNT)-water nanofluid respectively, in a plate heat exchanger. Farajollahi *et al.* [19] experimentally investigated on heat transfer coefficient of a shell and tube heat exchanger with Al<sub>2</sub>O<sub>3</sub>-water and TiO<sub>2</sub>-water nanofluid. Enhancement of heat transfer coefficient up to 56.0% has been obtained with both nanofluids compared with water. Yousefi *et al.* [20] measured the increase of thermal efficiency of a plate solar collector by using Al<sub>2</sub>O<sub>3</sub>-water nanofluid with weight fraction from 0.2% to 0.4%. Experimental results showed increase of 28.3% of efficiency with Al<sub>2</sub>O<sub>3</sub>-water at 0.2%wt. Also, thermal efficiency of the same plate solar collector with MWCNT at weight fraction from 0.2% to 0.4% as working fluid was investigated by Yousefi *et al.* [21], finding enhancement of thermal efficiency. For instance, at 0.4%wt of solid phase and flow rate of 0.05 kg/s enhancement up to about 20.0% has been obtained. Colangelo *et al.* [22] have built a modified plate solar collector to avoid sedimentation of solid phase and experimentally investigated on thermal efficiency by using water and Al<sub>2</sub>O<sub>3</sub>-water at 3.0%vol. Enhancement from about 7.0% to 10.0% have been obtained with nanofluid.

In electronic devices, thermal management is an important aspect to take into account because their performance is affected by temperature and technical life could be decreased by thermal stress.

Although typical size of electronic components and especially of microprocessors decreased in the last decades, electric power, which they absorb, increases according to their temperature.

Therefore, the challenges of thermal management in electronics devices is twofold: size reduction of heat transfer systems and improvement of their capabilities.

Different traditional technologies and techniques (passive and active) are used to guarantee efficient cooling to electronic devices and, in general, they can be grouped in: radiation and free convection, forced air cooling, forced liquid cooling, liquid evaporation. On the other hand, the most popular heat transfer fluids used in this field can be grouped in: gas (air), liquid, refrigerant (phase change) [23]. According to this classification, today, the most developing and studied technologies are focused mainly on: microchannels, heat pipes, heat pumps, spray cooling, phase change material, free cooling, thermoelectric cooling.

Tukerman *et al.* [24] in 1981 demonstrated that to enhance heat transfer coefficient of a heat sink it is possible to reduce characteristic width of the channel where coolant fluid flows, up to reach micrometric values. Actually, microchannel heat sinks (MCHSs), for capability to dissipate heat from electronic devices, are the first choice as electronic cooling systems [25]. The use of nanofluids in heat sinks for electronic devices may be another solution to be combined with MCHSs [26][27] to further improve their heat dissipation capability. The objective of this paper is to give to scientific community an overview on nanofluids applications in electronic cooling systems. Furthermore, this analysis has been carried out to be a useful tool to know the main results and the typical liquid/solid mixtures used and combined to technical and geometric solutions.

This review study is structured as follows: section 2 refers to papers focused on rectangular microchannel heat sinks, which are the most common type of MCHS; section 3 analyzes further geometries of MCHS; section 4 is related to pin fins heat sinks; and finally, in section 5, heat pipes for electronic applications have been analyzed.

## 2. Rectangular microchannel heat sink (RMCHS)

Generally, microstructure heat sinks are based on the same principles of macroscale heat exchangers for what concerns design and technology. Highly conductive materials, as copper and aluminum, are employed to fabricate channels and contact surfaces, taking into account optimization of the heat exchange surface necessary to maintain the systems at a fixed temperature. Several micro heat sinks were investigated with nanofluids, as working fluid, to analyze their thermal performance and any critical issue, as next reported.

Plate heat sinks, commonly employed in cooling of electronic devices, generally consist of a plane box, where electronic components are placed. To enhance thermal performance of a heat exchanger, one of the most used method is to extend the heat transfer surface with fins of different size and shape. On this way, it is important to evaluate fin design to find a good compromise between cost and efficiency [28]. Fin shape can be longitudinal, spine [29] or annular with the same material of the wall or with a higher thermally conductive material. Generally, heat sinks are made of copper, aluminum or silicon, therefore heat sink with fins is obtained by a single block.

Recently, literature has shown a large interest for heat sinks with longitudinal fins that form rectangular microchannels as the example in Figure 1 shows.

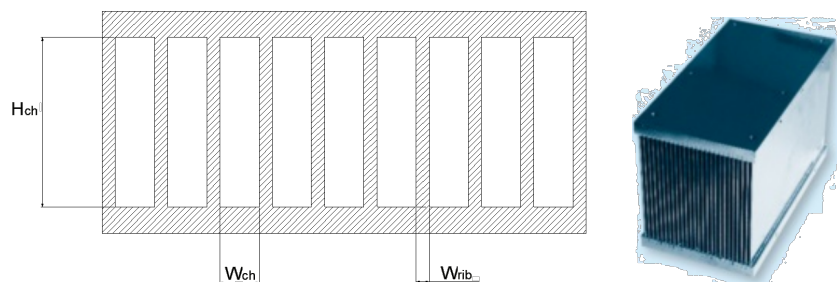


Figure 1. Rectangular Microchannel Heat Sink (RMCHS)

About this topic, in the following, several studies have been reported and analyzed, differentiating them in experimental and numerical works.

### 2.1. Experimental studies on RMCHS

Three different microchannel heat sinks were built by Escher *et al.* [30] with channel width ( $W_{ch}$ ) of 50, 100 and 200  $\mu\text{m}$ . Particularly, they experimentally investigated these sinks coupled with high volume fraction  $\text{SiO}_2$ -water nanofluids (5.0, 16.0 and 31.0%). Results showed that thermal resistance was independent from volume fraction for all heat sinks. Besides authors carried out a sensitivity analysis that demonstrated an increase in heat capacity of working fluid, promising to enhance heat sink performance.

Selvakumar *et al.* [31] investigated the effect of  $\text{CuO}$ -water nanofluid at a volume fraction of 0.1% and 0.2% respectively on a heat sink with 49 channels of length 28.0 mm, width 0.3 mm and height 2.0 mm. The bottom surface of the heat sink and fins were made of copper, whereas the top one of acrylic. Interface temperature, convective heat transfer coefficient and pressure drop were analyzed. At 0.2%vol, interface temperature was 1.15  $^\circ\text{C}$  lower than that measured with water, besides an increase of heat transfer coefficient of 29.63% was observed with nanofluid. The same heat sink was also studied with  $\text{Al}_2\text{O}_3$ - $\text{Cu}$ /water hybrid nanofluid at 0.1%vol and 0.0131 kg/s [32]. Interface temperature was 18.3  $^\circ\text{C}$  with water and 17.2  $^\circ\text{C}$  with nanofluid. Regarding convective heat transfer coefficient, enhancements up to 25.2% were obtained when nanofluid was used. By using  $\text{CuO}$ -water nanofluid, enhancement up to 70.0% of heat transfer coefficient and a decrease of thermal

resistance of 25.0% were obtained. Furthermore, Al<sub>2</sub>O<sub>3</sub>-water nanofluid at volume fraction up to 2.0% and Reynolds range between 226 and 1676, was experimentally investigated for a heat sink with 25 parallel rectangular microchannels, with a cross section of 283x800 μm and a length of 50 mm [33]. With the same closed loop used in [33], a heat sink with 10 parallel rectangular minichannels of length of 50 mm, height of 1.5 mm and width of 1 mm was investigated with Al<sub>2</sub>O<sub>3</sub>-water based nanofluids with a weight fraction up to 10% [34]. In this case, the heat sink was studied in a Reynolds range between 133 and 1515, obtaining heat transfer coefficient increase up to 72.0%.

The same experimental setup was used to investigate the effect of water based suspension with microencapsulated phase change material particles (MEPCM) and a mixture of MEPCM and Al<sub>2</sub>O<sub>3</sub> particles by Ho *et al.* [35]. The aim of this work was to find a correlation among experimental results and relevant parameters. A minichannel heat sink was tested in a range of mass fraction between 0 and 10%. Nusselt number, wall temperature control effectiveness and average thermal resistance reduction were investigated. Maximum error of the proposed correlations versus experimental results was 9.99% for Al<sub>2</sub>O<sub>3</sub>-water, 13.2% for mixture with Al<sub>2</sub>O<sub>3</sub> and 9.30% for MEPCM.

Nitiapiruk *et al.* [36] experimentally investigated a microchannel heat sink with TiO<sub>2</sub>-water nanofluids at volume fraction from 0.5% to 2.0%. Each microchannel had 500 μm width, 800 μm height and 40 mm length. When increasing volume fraction from 0.5% to 1.0% the heat transfer coefficient increased more than 500 W/m<sup>2</sup>K. From 1.5% to 2.0% enhancement of heat transfer coefficient was lower than 200 W/m<sup>2</sup>K. Higher gradient enhancement was obtained at low volume fraction, due to low viscous forces compared to other concentrations.

A 50x50x10 mm copper rectangular microchannel heat sink was experimentally investigated with Al<sub>2</sub>O<sub>3</sub>-water nanofluid at volume fraction from 0.10% to 0.25% and in flow range between 0.5 and 1.25 l/min [37]. Each channel had height of 0.8 mm and width of 0.5 mm. To simulate heat power yielded by electronic devices, two cartridges of 200 W were placed below the heat sink. The system was investigated with a Reynolds number between 395 and 989. By using nanofluids at 0.25 %vol a decrease of 1.4 °C of the heat sink base temperature, compared to water at the lowest Reynolds number, was observed. This decrease was 2.7 °C at the highest Reynolds number. Convective heat transfer coefficient increased up to 18% by using Al<sub>2</sub>O<sub>3</sub>-water nanofluids, whereas enhancement of 17.80% for Nusselt number and reduction of 15.72% for thermal resistance were observed. Thermal effectiveness increased with volume fraction as well. Regarding flow rate, at 0.10%vol and 0.15%vol, thermal effectiveness increased until flow rate was 0.75 l/min and after it decreased. At 0.20%vol and 0.25%vol, the maximum was reached with 0.875 l/min.

A single channel heat sink (SCHS) and a microchannel heat sink (MCHS) were experimentally investigated by Zhang *et al.* [38] using water, Al<sub>2</sub>O<sub>3</sub>-water and SiC-water nanofluids. For SCHS, negligible reduction of thermal resistance was observed by using SiC-water nanofluids. With Al<sub>2</sub>O<sub>3</sub>-water nanofluids at 4%vol, thermal resistance increased, reducing thermal performance of the heat sink. This behavior was due to sedimentation of solid phase. Experimental results, obtained with MCHS, showed decreases of thermal resistance up to 11% by using Al<sub>2</sub>O<sub>3</sub>-water nanofluids. However also high increases of pressure drop were observed with nanofluids for both SCHS and MCHS.

Jajja *et al.* [39] experimentally investigated 4 finned minichannel heat sinks with fin spacing of 0.2, 0.5, 1.0 and 1.5 mm, with MWCNT-water nanofluid at 1%wt as working fluid. Good results were obtained with 0.2 mm fin spacing and MWCNT as working fluid. Actually, the lowest heat sink base temperature was 49.7 °C, with MWCNT-water nanofluid at flow rate of 1 l/min. Besides, the overall heat transfer coefficient enhancement of 15% with MWCNT-water nanofluid and the lowest thermal resistance value of 0.049 K/W were recorded.

A heat sink obtained with a Cu-Be alloy block was experimentally investigated with CuO-water (0.1% and 0.2% volume fraction) and Al<sub>2</sub>O<sub>3</sub>-water (0.5% and 1.0% volume fraction) nanofluids by Peyghambarzadeh *et al.* [40]. Dimensions of the heat sink were 50 mm x 50 mm x 14 mm with 17

rectangular microchannels with cross section of 400x560  $\mu\text{m}$ . Enhancement of Nusselt number of 27% by using CuO-water at 0.2%vol was obtained. With  $\text{Al}_2\text{O}_3$ -water at 0.5%vol and 1.0%vol, Nusselt number increased of 28% and 49% respectively. From experimental results, it was possible to note that heat transfer coefficient reached with low concentrations of CuO (0.1% and 0.2%) was comparable with values obtained with  $\text{Al}_2\text{O}_3$  nanoparticles at higher concentration (0.5% and 1.0%). However, pressure drop was also comparable, therefore the advantage of using low concentration was nullified by pressure drop.

Ho *et al.* [41] studied a rectangular natural circulation loop that included 2 minichannel heat sinks as heated section and cooling section respectively. The heated section, with length of 50 mm and width of 48 mm, consisted in 23 minichannels with a hydraulic diameter of 0.96 mm. Besides, a heater to control wall temperature was placed at the bottom surface. Cooling section had 34 minichannels with the same hydraulic diameter of the heated section, with length of 105 mm and width of 58 mm. On the bottom side of heat sink a labyrinth channel path was realized, where water flew to maintain a constant wall temperature. Natural circulation loop was investigated with water and  $\text{Al}_2\text{O}_3$ -water nanofluids at weight fraction of 0.1%, 0.5% and 1.0%. Experimental results showed enhancement of heat transfer coefficient up to 22% for both minichannel heat sinks with a weight fraction of 1.0%.

## 2.2. Numerical studies on RMCHS

Jang *et al.* [42] numerically studied the performance of a heat sink working with water, Cu-water and Diamond-water nanofluids. They considered thermal conductivity of nanofluid based on Jang & Choi's model [43], volume fraction of 1.0%, Cu particles with a mean size of 6 nm and diamond particles with a mean size of 2 nm. The height of microchannel was 350 micrometers. Numerical simulation showed that by using nanofluids it is possible to reduce maximum temperature difference between heated microchannel wall and coolant. Besides this decrease was higher with diamond water nanofluid, determining a decrease of thermal resistance as well.

An analytical investigation on a 20x20 mm copper heat sink with rectangular minichannels with  $\text{TiO}_2$ -water and SiC-water nanofluids at 2 m/s and 6 m/s inlet velocity was carried out by Ijam *et al.* [44], while Xie *et al.* [45] numerically analyzed this heat sink with water. They found that thermal resistance was 0.035 W/K at 2 m/s, whereas at 6 m/s it was 0.0224 W/K. In this investigation, by using SiC-water nanofluids at 4% of volume fraction and with 2 m/s inlet velocity, thermal resistance was 0.0333 K/W, whereas at 6 m/s it was 0.01996 K/W. Similarly, by using  $\text{TiO}_2$ -water based nanofluid at 4% of volume fraction it was 0.0331 K/W at 2 m/s and 0.0199 K/W at 6 m/s.

A rectangular MCHS was numerically investigated to study its thermal performance with  $\text{Al}_2\text{O}_3$ -water nanofluid in a Reynolds range of 100-1000 [46]. In this case, fluid was considered as single phase in the numerical model. Heat flux was considered at the top plate of MCHS from 100 to 1000  $\text{W}/\text{m}^2$ . Nanofluids were employed with a volume fraction of 1.0, 2.5 and 5.0%. Results showed that heat transfer coefficient increased with increasing of volume fraction from 0 to 2.5% and then decreased. Increase of pressure drop with volume fraction was negligible, whereas differences in temperature profile inside microchannel between nanofluids and pure water were appreciable when heat flux was 1000  $\text{W}/\text{m}^2$ .

A rectangular MCHS modeled as fluid-saturated porous medium and its cooling performance were investigated by Chen *et al.* [47]. Particularly, water and  $\text{Al}_2\text{O}_3$ -water nanofluid with volume fraction between 1.0 and 5.0% as working fluids were considered. Numerical results showed that inertial effect was not influenced by temperature wall along microchannel, whereas fluid temperature was affected. Besides, average Nusselt number was directly proportional to volume fraction of solid phase.

An inverse problem optimization method was used to find the optimal geometry of a rectangular MCHS to minimize thermal resistance with  $\text{Al}_2\text{O}_3$ -water nanofluid and water as working fluids [48]. Optimization was made varying channel number (N), channel aspect ratio ( $\alpha = H_{\text{ch}}/W_{\text{ch}}$ ), ratio of width of channel to pitch ( $\beta = W_{\text{ch}}/(W_{\text{ch}} + W_{\text{rib}})$ ) at fixed pumping power. Results showed a

relationship between geometry and heat transfer fluid. With Al<sub>2</sub>O<sub>3</sub>-water nanofluid at 1.0 %vol, N=51,  $\alpha=5.69$  and  $\beta=0.62$ , thermal resistance was 0.106 K/W, whereas with water as working fluid N=95,  $\alpha=10.13$ ,  $\beta=0.66$ , thermal resistance was 0.148 K/W. Besides it was observed that thermal resistance was inversely proportional to pumping power. The same authors demonstrated that with 1.0%vol Al<sub>2</sub>O<sub>3</sub>-water nanofluid the optimal design had N=134,  $\alpha=6.39$  and  $\beta=0.37$ , with thermal resistance of 0.0876 K/W for flow rate of 200 cm<sup>3</sup>/min. At fixed pressure drop of 20 kPa optimal geometry was found for N=37,  $\alpha=4.38$  and  $\beta=0.59$ , with thermal resistance of 0.0760 K/W [49]. Therefore, optimal geometry depended on constrain conditions.

Forchheimer-Brickman-extended Darcy equation and the volume-averaged two equations model were used to investigate on thermal performance of a rectangular heat sink with SiO<sub>2</sub>-water based nanofluid as working fluid [50]. Results showed that heat transfer coefficient was proportional to porosity. Besides average enhancement of heat transfer coefficient was of 4.0, 5.5, 6.5 and 8.0% at 3.5, 4.0, 4.5 and 5.0% volume fraction, respectively.

Viscous effect along microchannels for a rectangular MCHS with Al<sub>2</sub>O<sub>3</sub>-water nanofluid was numerically studied by Lelea [51]. Volume fraction from 1.0 to 9.0% and 3 particle sizes (13, 28 and 47 nm) were considered for heating and cooling cases. For heating case, heat transfer coefficient enhancement up to 27% was calculated with volume fraction of 3.0% and particle size of 13 nm. With average particle size of 28 nm and 1.0 %vol nanoparticles concentration heat transfer enhancement was 5.0%, whereas for 47 nm it was less than 5.0%. Similar results for cooling case were obtained and heat transfer enhancement was inversely proportional to particle size.

Kamali *et al.* [52] numerically investigated thermal resistance variation and heat transfer coefficient of a rectangular MCHS varying heat transfer fluid. Particularly, a heat sink, with 26 microchannels with 280 x 430  $\mu\text{m}$  rectangular cross section and length of 1 cm, was considered. Water, Al<sub>2</sub>O<sub>3</sub>-water and MWCNT-water were the working fluids. Heat transfer enhancement up to 2.0% for Al<sub>2</sub>O<sub>3</sub>-water and 36.0% for MWCNT-water, compared with water, were obtained. Besides, mean thermal resistance reduction of 1.0% and 18.0% for Al<sub>2</sub>O<sub>3</sub>-water and MWCNT-water were found respectively.

The effect of Cu-water based nanofluids on thermal performance of 2 rectangular MCHS was investigated, according to an experimental correlation and a theoretical model respectively [53]. The authors demonstrated that nanoparticle thermal dispersion played a key role on reduction of thermal resistance of MCHS. For MCHS1 ( $W_{\text{ch}}=W_{\text{rib}}=100 \mu\text{m}$  and  $H_{\text{ch}}=300 \mu\text{m}$ ) thermal resistance achieved with pure water was 0.1803 K/[W cm<sup>2</sup>] with a pumping power of 3 W, whereas it was 0.085 K/W/cm<sup>2</sup> with Cu-water nanofluid at a volume fraction of 2.0%. At the same volume fraction and pumping power, thermal resistance was 0.06 K/W/cm<sup>2</sup> for MCHS2 ( $W_{\text{ch}}=W_{\text{rib}}=57 \mu\text{m}$  and  $H_{\text{ch}}=365 \mu\text{m}$ ).

SiC-water and TiO<sub>2</sub>-water nanofluids flowing inside a MCHS were numerically investigated for volume fraction from 0.8% to 4.0% in turbulent flow conditions [54]. Results showed that convective heat transfer coefficient was proportional to volume fraction and Reynolds number. Low differences were observed between results obtained with SiC and that with TiO<sub>2</sub>, whereas pumping power for SiC-water was higher than that for TiO<sub>2</sub>-water nanofluid.

Hung *et al.* [55] numerically studied the effect of nanofluids on a rectangular MCHS. CuO, Al<sub>2</sub>O<sub>3</sub>, Cu, TiO<sub>2</sub> and diamond nanoparticles were considered, whereas water, engine oil and ethylene glycol as base fluid. The best results were obtained with Al<sub>2</sub>O<sub>3</sub>-water. At the same fluid inlet temperature, lower local temperature difference between fluid and wall was obtained with Al<sub>2</sub>O<sub>3</sub>-water nanofluid, for low (1.0%) and high (5.0%) volume fractions. Besides thermal resistance decreased with increasing of volume fraction up to 1.0 % and 2.0% with pumping power of 0.05 W and 0.5 W respectively and then increased. The maximum decrease of thermal resistance compared to water was of 21.6% at 1.0 %vol.

A rectangular MCHS, in which each channel had height of 198  $\mu\text{m}$ , width of 59.85  $\mu\text{m}$  and length of 10 mm, was numerically investigated with Al<sub>2</sub>O<sub>3</sub>-water nanofluid as working fluid with a volume fraction from 1.0 to 4.0% by Nebbati *et al.* [56]. On the bottom surface of MCHS a constant heat

flux from 300 to 1200 kW/m<sup>2</sup> was considered. Results showed that average Nusselt number increased with volume fraction and Reynolds number. Enhancement was about 20.0% for each volume fraction compared with Nusselt number calculated with water.

An analytical study was made to investigate and optimize thermal performance of a rectangular MCHS with Cu-water and CNT-water nanofluid as working fluid by Tsai *et al.* [57]. MCHS was considered as porous medium and results showed that the best geometry was obtained when the aspect ratio was  $\alpha_s = H_{ch}/W_{ch} = 6.4$ . Besides thermal resistance of MCHS was 0.086 °C/W for water, 0.0657 °C/W for Cu-water at 4.0%vol and 0.0642 °C/W for CNT-water respectively.

### 2.3. Final consideration on rectangular MCHS

Table 1 summarizes thermal resistance reduction, heat transfer coefficient enhancement and Nusselt enhancement for some rectangular MCHSs (those with the most significant results) at fixed volume fraction, analyzed in this section. It is possible to note a dispersion of both experimental and numerical results. This means that thermal performance of MCHS depends not only on nanofluid properties, but also on MCHS geometry.

Table 1. Experimental and numerical results at fixed volume fraction for the most significant MCHSs of this section

Reference	Nanofluid	Particle size [nm]	Nu enhancement	R <sub>T</sub> reduction [%]	h enhancement [%]	Method
Selvakumar <i>et al.</i> [31] - 2012	CuO-water (0.2%vol)	27-37	N.A.	N.A.	29.63	Experimental
Selvakumar <i>et al.</i> [32] - 2012	Al <sub>2</sub> O <sub>3</sub> -Cu-water (0.1%vol)	17	N.A.	N.A.	25.20	Experimental
Ho <i>et al.</i> [33] - 2010	Al <sub>2</sub> O <sub>3</sub> -water (2.0%vol)	33	N.A.	25.00	70.00	Experimental
Ho <i>et al.</i> [34] - 2013	Al <sub>2</sub> O <sub>3</sub> -water (10.0%wt)	33	N.A.	N.A.	72.00	Experimental
Nitiapiruk <i>et al.</i> [36] - 2013	TiO <sub>2</sub> -water (2.0%vol)	N.A.	24.70 (at Re=400 and heat flux of 50.6 W) 15.49 (at Re=1200 and heat flux of 50.6 W)	N.A.	N.A.	Experimental
Sohel <i>et al.</i> [37] - 2014	Al <sub>2</sub> O <sub>3</sub> -water (0.25%vol)	13	17.80	15.72	18.00	Experimental
Zhang <i>et al.</i> [38] - 2009	Al <sub>2</sub> O <sub>3</sub> -water (4.0%vol)	60	N.A.	11.00	N.A.	Experimental
Jajja <i>et al.</i> [39] - 2014	MWCNT-water (1.0%wt)	N.A.	N.A.	N.A.	15.00	Experimental
Peyghambarzadeh <i>et al.</i> [40] - 2014	Al <sub>2</sub> O <sub>3</sub> -water (1.0%vol)	20	N.A.	N.A.	49.00	Experimental
	CuO-water (0.2%vol)	40	N.A.	N.A.	27.00	
Ho <i>et al.</i> [41] - 2014	Al <sub>2</sub> O <sub>3</sub> -water (1.0%wt)	85-100	N.A.	N.A.	22.00	Experimental
Ijam <i>et al.</i> [42] - 2012	TiO <sub>2</sub> -water (4.0%vol)	N.A.	N.A.	5.40 (at 2.0 m/s) 11.16 (at 6.0 m/s)	N.A.	Analytical
	SiC-water (4.0%vol)	N.A.	N.A.	4.80 (at 2.0 m/s) 10.89 (at 6.0 m/s)	N.A.	
Hosseini Haschemi	SiO <sub>2</sub> -water	N.A.	N.A.	N.A.	8.0	Numerical



<i>et al.</i> [50] - 2012	(5.0%vol)					
Lelea [51] - 2011	Al <sub>2</sub> O <sub>3</sub> -water (3.0%vol)	13	N.A.	N.A.	27.00	Numerical
	Al <sub>2</sub> O <sub>3</sub> -water (1.0%vol)	28	N.A.	N.A.	5.00	
	Al <sub>2</sub> O <sub>3</sub> -water (1.0%vol)	47	N.A.	N.A.	< 5.00	
Kamali <i>et al.</i> [52] - 2013	Al <sub>2</sub> O <sub>3</sub> -water (0.921%vol)	N.A.	N.A.	1.00	2.00	Numerical
	MWCNT- water (0.921%vol)	N.A.	N.A.	18.00	36.00	
Chein <i>et al.</i> [53] - 2005	Cu-water (2.0%vol)	N.A.	N.A.	52.85	N.A.	Analytical
Hung <i>et al.</i> [55] - 2012	Al <sub>2</sub> O <sub>3</sub> -water (1.0%vol)	38.4	N.A.	21.60	N.A.	Numerical
Nebbati <i>et al.</i> [56] - 2015	Al <sub>2</sub> O <sub>3</sub> -water (from 1.0 to 4.0%vol)	N.A.	20.00	N.A.	N.A.	Numerical
Tsai <i>et al.</i> [57] - 2007	Cu-water (4.0%vol)	N.A.	N.A.	23.60	N.A.	Analytical
	CNT-water (4.0%vol)	N.A.	N.A.	25.34	N.A.	

Results of this section show a reasonable advantage in using nanofluids in RMCHS. Even if the explored investigations cover only partially the possibility of nanofluids, it is clear that the most used nanoparticles are Al<sub>2</sub>O<sub>3</sub>. This is due to their peculiar characteristics under thermo-physical and economic points of view. Actually, these nanoparticles are one of the cheapest on the market and offer good performance and excellent stability. In all the examined works, there are no data about the problem of clogging and how to face it. It could be a big issue, particularly for high concentration of nanoparticles as in [38][50][56][57]. The results and conclusions of those works have to be reconsidered after further considerations about the real possibility and convenience to use high concentration of nanoparticles, in particular for concentrations higher than 1.0%vol.

### 3. Different geometries of MCHS

Although rectangular MCHS are the most studied types of microstructure heat sinks, in literature several alternative geometries are described and analyzed. Therefore, in this section, these papers have been classified and their results analyzed in depth.

#### 3.1. Commercial MCHS

Some authors have directly used nanofluids in commercial heat sinks to investigate temperature on the contact surface or heat transfer coefficient. Thang *et al.* [58] used CNTs with an ethylene glycol/water solution in a heat sink attached on an Intel Core i5 processor to dissipate heat, generated during full load operation. The first comparison was made between temperature of the microprocessor reached with a traditional cooling fan and that obtained with heat sink and EG/DW solution as working fluid. The saturation temperature decreased of about 14 °C using heat sink with EG/DW only as heat transfer fluid, while when experimental setup was tested with nanofluid, saturation temperature decreased of about 20 °C. Korpyś *et al.* [59] studied the influence of CuO-water nanofluid with a volume fraction from 0.86% to 2.25% on a commercial heat sink (ZM-WB3 Gold by Zaman) fixed to the Intel Pentium 4 HT 570J CPU, which dissipates 115 W. Mass flow rate was between 0.009 and 0.05 kg/s. The best result was obtained with CuO-water nanofluid at 2.25 %vol. Temperature of CPU was 0.5 °C lower than that obtained with water as working fluid. Turgut *et al.* [60] investigated on performance of a commercial liquid cooling kit (Coolermaster

Seidon 120M), with a water block attached on a heater, that simulated heat yielded by a CPU, with water and Al<sub>2</sub>O<sub>3</sub>-water nanofluid at 1.0% of volume fraction. With Al<sub>2</sub>O<sub>3</sub>-water the temperature reached on the contact surface between water block and heater was 6.7% lower than that with water. Another commercial liquid cooling system (Thermal Take Bigwater 760is) was investigated by Roberts *et al.* [61] with water and Al<sub>2</sub>O<sub>3</sub>-water nanofluid at a volume fraction of 0.1%, 0.5% and 1.0%. A convective heat transfer enhancement of 18.0% was obtained with 1.0%vol Al<sub>2</sub>O<sub>3</sub>-water. Rafati *et al.* [62] tested the 3D Galaxy II (Gigabyte) liquid cooling kit on a Phenom II X4 965 with SiO<sub>2</sub>, TiO<sub>2</sub> and Al<sub>2</sub>O<sub>3</sub> water based nanofluids at a flow rate from 0.5 to 1.0 l/min. Lower processor operating temperatures were observed with Al<sub>2</sub>O<sub>3</sub>-water nanofluids. For instance, at 0.5%vol and 1.0 l/min temperature was about 46.8 °C, 46.5 °C and 45.0 °C with SiO<sub>2</sub>, TiO<sub>2</sub> and Al<sub>2</sub>O<sub>3</sub> water based nanofluid respectively. Figure 2 shows the commercial heat sinks under investigation.

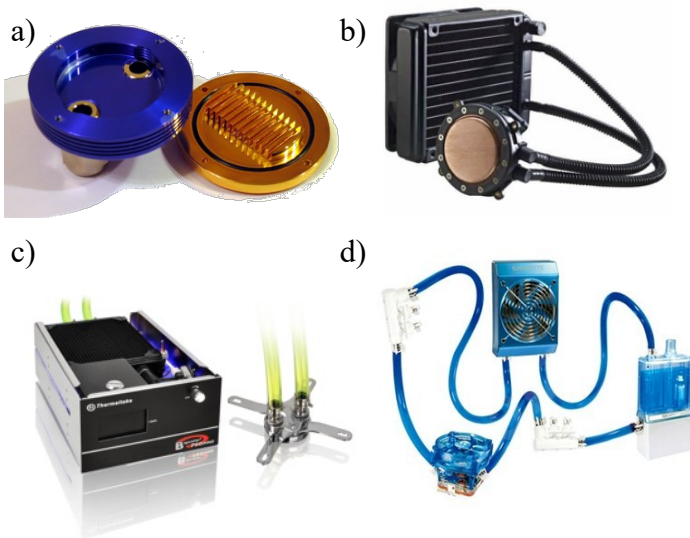


Figure 2. Commercial heat sinks: a) ZM-WB3 Gold; b) CoolerMaster Seidon 120M; c) Thermal Take Bigwater 760is; d) 3D Galaxy II

### 3.2. Trapezoidal MCHS

The most popular MCHSs have channels with rectangular cross section, but literature also deals with other types of microchannels, as trapezoidal ones, and their thermal performance with nanofluids. A simple scheme of this kind of MCHS is reported in Figure 3.

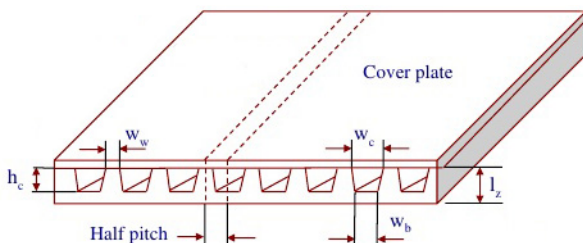


Figure 3. Scheme of trapezoidal MCHS

Chein *et al.* [63] experimentally investigated a trapezoidal MCHS with water and Cu-water nanofluid with volume fraction from 0.2 to 0.4%. Flow rates were 10, 15 and 20 ml/min for all fluids. Results showed that energy absorbed by the fluid increased with increasing of volume fraction of solid phase until flow rate was lower than 15 ml/min. Over this value the effect of nanoparticles was negligible. Thermal resistance decreased as flow rate increased up to 15 ml/min.

However, when flow rate was 20 ml/min thermal resistance with nanofluids was higher than that with water. This behavior implies a worsening of the performance of the heat sink due to clustering and sedimentation phenomena at high flow rate. A numerical investigation was made by Fani *et al.* [64] to study the effect of particle size on thermal performance of a trapezoidal MCHS, with CuO-water nanofluid at laminar conditions. Particle size range used in this study was from 100 nm to 200 nm. Pressure drop and pumping power increased with increasing of particle size. For instance, for particle size of 200 nm pressure drop was 15% higher than that obtained with 100 nm. Besides, Nusselt number was inversely proportional to particle size. At  $Re=500$  and volume fraction of 4.0%, Nusselt number obtained with particle size of 200 nm was 17.6% lower than that obtained with 100 nm. Mohammed *et al.* [65] investigated on thermal performance of a trapezoidal MCHS using various nanofluids based on water, ethylene glycol, oil and glycerin as base fluid respectively. Solid phase consisted in 2% volume fraction of diamond nanoparticles. Besides various materials were considered for MCHS, in particular: copper, aluminum, steel and titanium respectively. At a fixed MCHS material a better heat transfer coefficient was obtained with Glycerin-diamond nanofluids, while lower values were obtained with water-diamond nanofluid. Therefore, at fixed heat transfer fluid, using steel as MCHS material, heat transfer coefficient of water based nanofluid can be enhanced, whereas for other nanofluids, enhancement can be obtained with copper MCHS. These behaviors show that thermal diffusivity of MCHS material plays a key role for heat transfer inside MCHS.

### 3.3. Triangular MCHS

Mohammed *et al.* [66] numerically investigated, as well, the impact of various nanofluids on thermal performance of a triangular aluminum MCHS, whose scheme is reported in Figure 4.

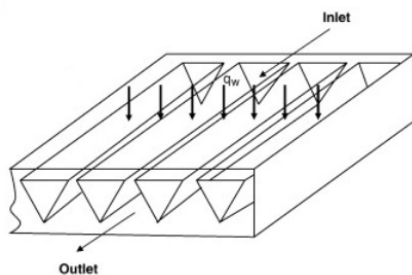


Figure 4. Scheme of triangular MCHS

Water based nanofluids with 2% of volume fraction of  $Al_2O_3$ , Ag, CuO, diamond,  $SiO_2$  and  $TiO_2$  were studied. Numerical results showed that the highest heat transfer coefficient was obtained with diamond-water nanofluid, whereas the lowest value was obtained with  $Al_2O_3$ -water. Besides, using  $SiO_2$  nanoparticles the highest values of pressure drop was obtained.

### 3.4. Circular microchannel heat sink

Fazeli *et al.* [67] experimentally investigated an aluminum heat sink (40x40x8.5 mm) with 5 circular channels of diameter equal to 4.0 mm. Water and  $SiO_2$ -water nanofluids were used as working fluid. Heat transfer coefficient increases of 3-8%, 8-8.5%, 10.5-13.0% and 9-15.0% with a volume fraction of 3.5, 4.0, 4.5 and 5.0% were obtained, respectively. Heat sink performance with magnetic nanofluids (mixtures of water and  $Fe_3O_4$  nanoparticles at a volume fraction of 0.5, 1.0, 2.0 and 3.0%) under the effect of a magnetic field was investigated by Ashjaee *et al.* [68]. A heat sink with dimensions of 40 mm x 40 mm x 10 mm and with 5 circular channels with diameter of 4 mm and length of 40 mm was placed between the tips of an electromagnet that yielded a magnetic field lower than 1.4 G. Heat transfer coefficient and Nusselt number, at laminar conditions and a heat flux of  $66000 \text{ W/m}^2$ , obtained through a heater installed on the bottom surface of heat sink, were calculated. Heat transfer coefficient increased with increasing of volume fraction and

Reynolds number. In absence of magnetic field, enhancement up to 14% was observed compared with water. Instead, with magnetic field, heat transfer coefficient reached enhancement of 38%. An optimum magnetic flux density of 400 G was found for high concentration with which maximum efficiency was obtained.

Mital [69] through semi-empirical correlations analyzed thermal resistance of a heat sink with circular channels with diameter of 0.1 mm and water and Al<sub>2</sub>O<sub>3</sub>-water nanofluid, as working fluid. Results showed that at low levels of pumping power a small decrease in thermal resistance by using nanofluid was obtained. Actually, at 0.1, 0.5 and 0.9 W of pumping power, thermal resistance with nanofluid was only 0.003 °C/W lower than that calculated with water. On the other hand, at higher level of pumping power this difference was 0.002 °C/W. Therefore, adding nanoparticles small benefits can be obtained because solid phase increases power consumptions of the cooling system.

### 3.5. Complex MCHS

A complex microchannel heat sink with Al<sub>2</sub>O<sub>3</sub>-water nanofluid and water as working fluids was studied by Zhai *et al.* [70]. Volume fraction of solid phase was 0.5% and 1.0%, whereas Reynolds number ranged between 100 and 700. The heat sink consisted of 10 microchannels with cavities along longitudinal axis and dimensions as shown in Figure 5.

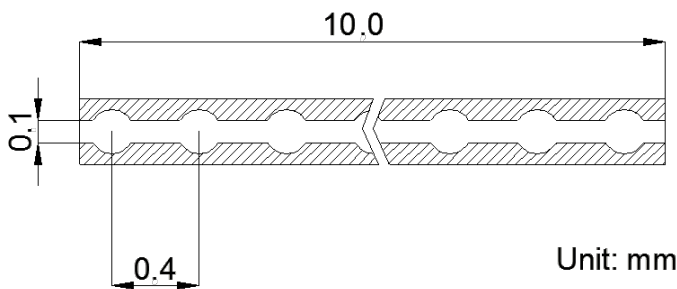


Figure 5. Channel of MCHS with cavities

Thermal resistance was inversely proportional to Reynolds number and volume fraction, while Nusselt number and friction factor increased with Reynolds number and volume fraction. For instance, at Re=658 and volume fraction of 1.0% Nusselt number and friction factor increased of 1.4 and 1.7 times respectively, compared to water. Performance of complex microchannels heat sink with nanofluid were compared with those of a smooth microchannels (without cavities) with water. At 1.0% of volume fraction and Re=658, thermal resistance decrease was 22.5% lower than that obtained with water and smooth microchannels. An interrupted microchannel heat sink (IMCHS) was numerically investigated by Mat Tokit *et al.* [71] to study the effect of nanofluids on thermal performance. Al<sub>2</sub>O<sub>3</sub>, CuO and SiO<sub>2</sub> nanoparticles and water were considered as solid and liquid phase respectively, whereas particles size was from 30 to 60 nm and volume fraction from 1.0 to 4.0%. IMCHS was investigated with Reynolds number from 140 to 1034. Numerical results showed that at Re=140 and particle size of 30 nm average, Nusselt number at 4.0%vol increased of 163.9%, 11.1% and 9.4% for SiO<sub>2</sub>, Al<sub>2</sub>O<sub>3</sub> and CuO water based nanofluid respectively. Besides, average Nusselt number was directly proportional to volume fraction and inversely proportional to particle size. For instance, with Al<sub>2</sub>O<sub>3</sub>-water at 3.0%vol an enhancement of 3.0% of Nusselt number was obtained for particle size of 60 nm, whereas this increase was of about 5.5% for 30 nm.

Kuppusamy *et al.* [72] numerically investigated the effect of nanofluid inside a triangular grooved microchannel heat sink (TGMCHS). Among CuO, ZnO, Al<sub>2</sub>O<sub>3</sub> and SiO<sub>2</sub> solid phases, the best thermal performance was obtained with Al<sub>2</sub>O<sub>3</sub>. For instance, a Nusselt number enhancement of 14.8% was observed with Al<sub>2</sub>O<sub>3</sub>-water at 1.0%vol. Analogously a decrement of 5.0% of thermal resistance was obtained.

Farsad *et al.* [73] numerically investigated the effect of nanofluid on thermal performance of an irregular heat sink. Al<sub>2</sub>O<sub>3</sub>, CuO and Cu nanoparticles were considered as solid phase with a volume

fraction up to 8.0% and water as liquid phase. Numerical simulations were carried out with FLUENT and showed that good results could be obtained with Cu-water nanofluids. Actually, at fixed volume fraction of 8.0% average heat transfer coefficient was 893 W/m<sup>2</sup>K for Al<sub>2</sub>O<sub>3</sub>, 894 W/m<sup>2</sup>K for CuO and 970 W/m<sup>2</sup>K for Cu. Besides heat transfer coefficient increased with flow rate and volume fraction.

A trapezoidal grooved MCHS, as in Figure 6, was numerically investigated to find optimal geometry and to study influence of nanofluid on thermal performance [74]. Numerical results showed that the best results were obtained with  $a=40\ \mu\text{m}$  and  $Re=532.24$ . At these values, average Nusselt number enhancement was 95% and thermal resistance enhancement was 57%, compared with rectangular channel. Optimal  $b$  value was  $100\ \mu\text{m}$ , at  $a=40\ \mu\text{m}$  and pitch of  $450\ \mu\text{m}$ . Lower thermal resistance value was obtained for  $p_{\text{trap}}=400\ \mu\text{m}$ , with  $a=40\ \mu\text{m}$  and  $b=100\ \mu\text{m}$ . Actually, in this case average Nusselt number enhancement was 220%, compared with rectangular channel at  $Re=532.24$ . CuO, ZnO, Al<sub>2</sub>O<sub>3</sub> and SiO<sub>2</sub> nanoparticles were considered as solid phase for nanofluids with a volume fraction from 1.0 to 4.0%. Numerical results showed that with Al<sub>2</sub>O<sub>3</sub> nanofluid high heat transfer rate can be obtained. Besides, considering a particle size of 25 nm and a volume fraction of 4.0%, a thermal resistance decrease of 8.0% was observed and generally thermal resistance increased with particle size and decreased with volume fraction.

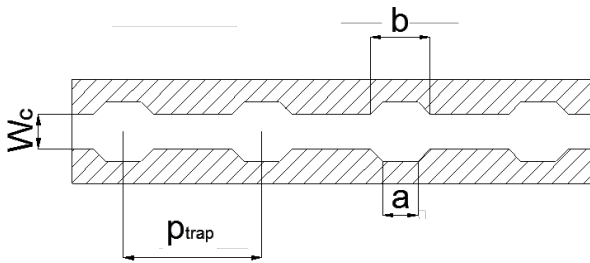


Figure 6. Channel of a trapezoidal grooved MCHS

Wavy microchannel heat sink with nanofluids was numerically investigated by Sakanova *et al.* [75]. Obtained results were compared with those of a rectangular microchannel heat sink. Microchannel with height of  $600\ \mu\text{m}$ , width of  $85\ \mu\text{m}$  and length of  $10\ \text{mm}$  were considered. The effect of nanofluids on performance of wavy microchannel heat sink was studied considering diamond nanoparticles as solid phase at a Reynolds number from 99 to 232. Numerical results showed that wavy channel increased heat transfer coefficient of heat sink compared to rectangular channel when working fluid was water. Furthermore, with a volume fraction of 1.0% at low Reynolds number, improvement in thermal resistance between 8.52 and 10.86%, compared with water, was obtained. At high Reynolds number, enhancement reached 24.1%. Instead improvement of thermal resistance for diamond-water nanofluids at volume fraction from 2.0 to 5.0% was negligible, compared to that obtained with 1.0% vol. Khoshvaght-Aliabadi *et al.* [76] experimentally investigated the effect of Al<sub>2</sub>O<sub>3</sub>-water nanofluid on a corrugated minichannel heat sink (CMCHS). Thermal performance of CMCHS was better than rectangular MCHS. Reduction of base temperature up to  $4.8\ ^\circ\text{C}$  with corrugated minichannel compared to straight minichannel was obtained. This variation has to be added to that of nanofluids, Al<sub>2</sub>O<sub>3</sub>-water, that enhanced performance of CMCHS. For instance, average thermal resistance decrement of 15.2% with nanofluid at 0.3% of weight fraction was obtained inside a CMCHS with wave-length of  $40\ \text{mm}$  and wave amplitude of  $1\ \text{mm}$ .

### 3.6. Wide MCHS

Another type of heat sink for electronic device is the wide microchannel heat sink that generally consists in a single channel with much larger width than height. Izadi *et al.* [77] numerically studied the axial conduction effect on a parallel plate MCHS with Al<sub>2</sub>O<sub>3</sub>-water nanofluid as working fluid. Results showed not uniform flux along axial direction of heat sink and this behavior was more emphasized when wall thickness of heat sink increased. Besides, by numerical study, average heat

transfer coefficient inversely proportional to wall thickness was obtained. Increase of volume fraction determined an enhancement of heat transfer coefficient along microchannel, but this behavior was more accentuated at low Reynolds number. Thermal resistance decreased with increasing of thermal conductivity of heat sink material. Effect of Al<sub>2</sub>O<sub>3</sub>-water nanofluid on a wide microchannel was investigated numerically and experimentally by Kalteh *et al.* [78]. The dimensions of microchannel were 94.3 mm length, 28.1 mm width and 0.580 mm height. From experimental results it was observed that Nusselt number increased with volume fraction in laminar conditions. At 0.2%vol, Nusselt number was about 20.0% higher than that calculated with water as working fluid. Rimbault *et al.* [79] studied hydraulic and thermal performance of a rectangular microchannel with height of 1.116 mm and width of 25.229 mm, with CuO-water nanofluids at volume fraction of 0.24, 1.03 and 4.5% respectively, in laminar and turbulent flow conditions. Pressure drop increase up to 70% was found, whereas heat transfer coefficient slightly increased at 0.24% and 1.03%. At 4.50% it was lower than that measured with water. Therefore, in this case, no significant enhancement has been obtained with nanofluids. Radwan *et al.* [80] numerically investigated a microchannel heat sink for low concentrated photovoltaic-thermal (LCPV/T) system, considering water, Al<sub>2</sub>O<sub>3</sub>-water and SiC-water nanofluids as working fluids. The height of the heat sink was 100 micrometers, while the length was 250 times the height. The concentration ratio, CR, considered in this study was from 1 to 40. The temperature of the solar cell decreased with volume fraction for both Al<sub>2</sub>O<sub>3</sub>-water and SiC-water nanofluids. However higher decrease of temperature of the cell was obtained with SiC nanoparticles. Furthermore, at CR less than 17.8 it was directly proportional to Reynolds number, whereas for CR greater than 17.8 an increase of Reynolds number determined a decrease of thermal efficiency of the heat sink. A parallel plate channel with height of 15 mm and length of 100 mm was numerically investigated by Namburu *et al.* [81]. CuO-water based nanofluid as working fluid with a range volume fraction between 2.0 and 10.0% was considered. Results showed that local Nusselt number was directly proportional to volume concentration and at 2.0 %vol an enhancement of 100% was obtained. Average Nusselt number increased of 3.8 times at 10.0%vol for Reynolds number from 100 to 2000. Furthermore, heat transfer coefficient increased with increasing of volume fraction. At Re=2000 heat transfer coefficient for water was 2930 W/m<sup>2</sup>K and for CuO-water nanofluid at 10%vol it was 7378 W/m<sup>2</sup>K. However high pumping power increase was found such that CuO-water nanofluids could be employed with volume concentrations up to 2.0%.

### 3.7. Cylindrical MCHS

To cool down electronic devices, it is often necessary to build heat sink with particular and dedicated geometry, as the system explained by Azizi *et al.* [82]. It was a cylindrical MCHS and it consisted in 86 rectangular microchannels with a hydraulic diameter of 0.560 mm. A cartridge heater was installed axially inside to simulate heat power generated by an electronic device and it was incorporated in a Plexiglas cover. Cu-water nanofluid and water were used as working fluid. Weight fraction of solid phase of nanofluids was 0.05%, 0.1% and 0.3% and heat flux of cartridge heater was 35 and 50 kW/m<sup>2</sup>. Flow rate was maintained below 2 l/min. It was observed that convective heat transfer coefficient was proportional to Reynolds number and concentration of solid phase. Values up to 13000 W/m<sup>2</sup>K were obtained. Nusselt number was also proportionally to weight fraction of solid phase. For instance, enhancements up to 17%, 20% and 23% for weight fraction of 0.05%, 0.1% and 0.3% respectively, compared with water, were obtained. However, it was not a monotonic function of Reynolds number. Actually, in laminar conditions, Nusselt number trend had a maximum point as well as effectiveness of the cylindrical microchannel heat sink. Besides pressure drop was less than 0.15 bar.

Azizi *et al.* [83] studied the effect of Cu-water nanofluid on thermal resistance with a weight fraction from 0.05% to 0.3% on cylindrical MCHS. Thermal resistance decreased with increasing of Reynolds number and weight fraction of solid phase. The maximum reduction was of 21.0% at 0.3%wt compared with water. Besides it was observed that at the inlet of microchannel



enhancements up to 43% of Nusselt number were obtained and heat transfer coefficient increased of 80% compared with water. Instead, at fully developed region, heat transfer coefficient improved of 16%.

### 3.8. Dedicated geometry of MCHS

Ahamed *et al.* [84] experimentally investigated performance of a Bismuth Telluride ( $\text{BiTe}_3$ ) thermoelectric cooler (TEC) coupled with a multiport minichannel heat exchanger (Figure 7) and  $\text{Al}_2\text{O}_3$ -water nanofluids as coolant.

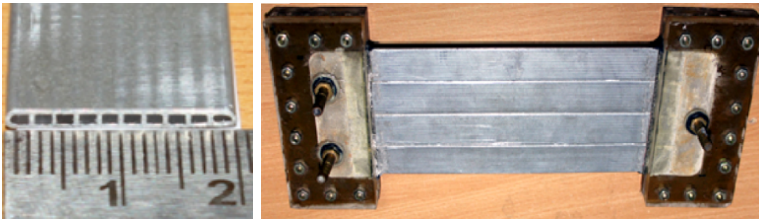


Figure 7. Photographs of the multiport minichannel heat exchanger [84]

Cold side of thermoelectric cooler was attached to an aluminum liquid cabin, while hot side to a multiport minichannel heat exchanger. The experimental campaign was carried out using water,  $\text{Al}_2\text{O}_3$ -water nanofluid at 0.1% and 0.2% volume fraction. Coefficient of performance of thermoelectric module (COP), thermal resistance between hot side and multiport minichannel, Nusselt number into minichannels with various coolant fluids were analyzed. COP and Nusselt number increased with volume fraction of solid phase. With an input power at the TEC of 400 W, the local Nusselt number showed an increase of 19.22% and 23.92% for 0.1%vol and 0.2%vol, compared with water at Reynolds number of 1000. Thermal resistance was inversely proportional to volume fraction of solid phase. This behavior determined an enhancement of performance of the system. However, pressure drop and pumping power increased also proportionally to volume fraction of solid phase. Actually, the enhancement of pressure drop was 31.58% with a volume fraction of 0.2% at Reynolds number of 1000, while pumping power increased of 41.29%.

An experimental investigation on base temperature, heat transfer coefficient and thermal resistance into a copper water block (Figure 8) with water and 0.1%vol  $\text{TiO}_2$ -water nanofluid was carried out by Khaleduzzaman *et al.* [85].

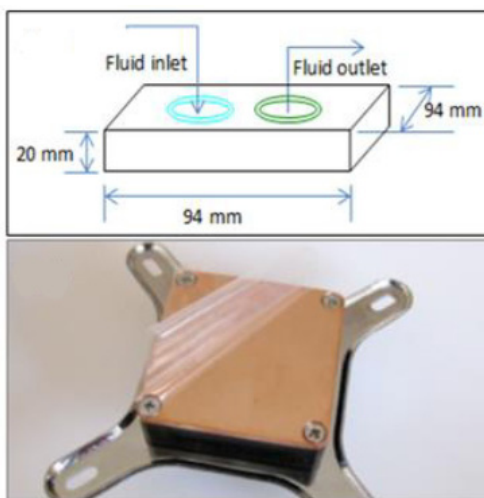


Figure 8. Copper water block [85]

Base temperature with nanofluid was lower than  $6.4\text{ }^{\circ}\text{C}$  compared with water at  $1.0\text{ l/min}$ . At  $1.5\text{ l/min}$  temperature gain was  $2.17\text{ }^{\circ}\text{C}$ . At  $1.5\text{ l/min}$ , thermal resistance was about  $0.10\text{ }^{\circ}\text{C/W}$  with water, whereas by using  $\text{TiO}_2$ -water nanofluid it was about  $0.08\text{ }^{\circ}\text{C/W}$ . Heat transfer coefficient enhancement was about  $10.5\%$ .

### 3.9. Spray/vapor MCHS

Heat transfer during spray cooling was studied by Khatak *et al.* [86]. For this purpose, an experimental setup was built to investigate temperature of heat transfer surface and heat flux. The liquid was dispersed on heat transfer surface in form of drops that evaporated, removing heat. Heat transfer surface was a part of copper cylindrical block where 4 cartridge heaters were placed as heat source. By experimental investigation it was observed a complete evaporation of the water at a flow rate of  $25\text{ ml/min}$  and a heating power of  $140\text{ W}$ . Therefore, to enhance the effectiveness of the system,  $\text{ZnO}$ -water nanofluids was used as cooling fluid. With this heat transfer fluid an increase of heat flux of  $20.2\%$  and a decrease of surface temperature of  $15\%$  were obtained with  $180\text{ W}$  heat input.

Jeng *et al.* [87] experimentally studied the effect of  $\text{Al}_2\text{O}_3$ -water nanofluid at  $1\%$ wt on a hybrid cooling system for electronics chips, consisting of a liquid cooling system and a vapor compression refrigeration system (VCRS) (Figure 9).

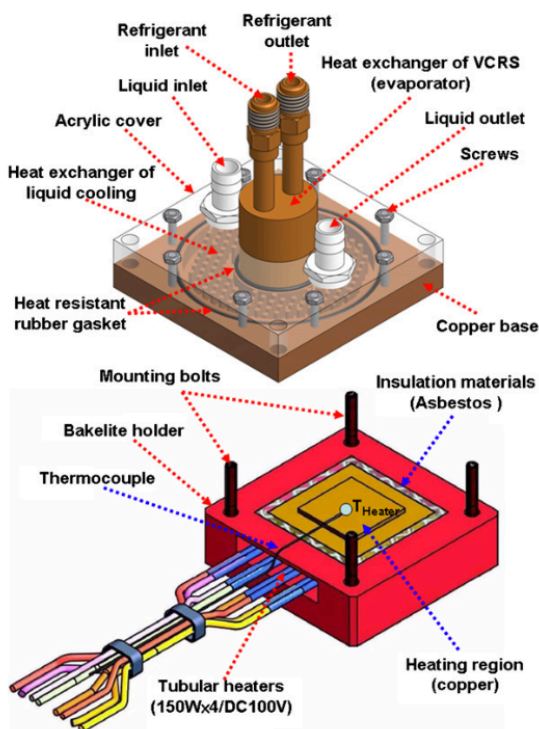


Figure 9. Structural diagram of the hybrid heat exchanger and heating module studied by Jeng *et al.* [87]

Hybrid cooling system was attached to a heating module that simulated a CPU at different power levels. Temperature of heater and power consumption at different operating conditions were investigated. The working fluid of cooling systems were water or nanofluid, while for VCRS it was a mixture of R290/R600a. Experimental results showed that at the maximum cooling capacity, heater surface temperature of  $80\text{ }^{\circ}\text{C}$  and pump power consumption of  $6.43\text{ W}$  were reached with water, while with nanofluid as working fluid, heater surface temperature was  $77.6\text{ }^{\circ}\text{C}$ , with the same power consumption. This behavior means that nanofluid increased the performance of cooling system.



Putra *et al.* [88] investigated the performance of a vapor chamber for electronic cooling systems with  $\text{Al}_2\text{O}_3$  water based nanofluid as working fluid. The vapor chamber was made with sintered copper powder, while the evaporator and condenser thickness were equal to 1.2 and 2 mm respectively. It was placed in a container, covered with a top plate and attached to a heat sink through the top plate and to a CPU on the side of the container. Charge volume ratio of the working fluid injected in vapor chamber was 60%. The system was tested with nanofluids at a volume fraction of 0.1%, 0.3%, 0.5%, 1.0%, 2% and 3%. Vapor chamber performance was investigated at full load condition and no load condition of CPU. Good results were obtained at full load condition and particularly at high concentration of solid phase. For instance, at 3%vol, average CPU temperature was  $54.64^\circ\text{C}$ , while the temperature obtained with water as working fluid was about  $60^\circ\text{C}$ . The effect of inclination angle of vapor chamber was investigated too. Better results were obtained for an inclination angle of  $0^\circ$  for all volume fractions of solid phase. At 2% nanofluid concentration, average temperature of CPU at horizontal position was  $56.06^\circ\text{C}$  and at  $45^\circ$  it was  $56.34^\circ\text{C}$ .

### 3.10. Enclosure MCHS

A numerical investigation on an enclosure as in Figure 13 with a heat sink and CuO-water nanofluid was made by Haasan [89]. The enclosure was considered in horizontal and vertical position respectively, Nusselt number was calculated varying the number of fins, ratio L/H, Rayleigh number, particles size and volume fraction of solid phase. A constant heat flux was considered at the bottom surface, while the top surface was maintained at constant temperature. Average Nusselt number increased with Rayleigh number, volume fraction and with decreasing of particle size for both horizontal and vertical position. For instance, with seven fins heat sinks, volume fraction of 1.0%, horizontal position and particle size of 10 nm, average Nusselt number enhancements of 110% at L/H of 0.25 and 40.0% at L/H of 0.5 were obtained.

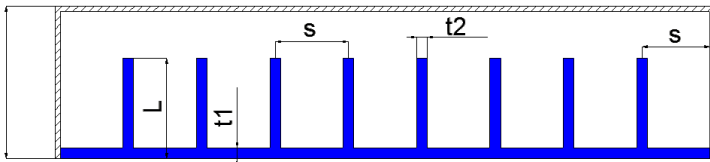


Figure 10. Enclosure heat sink

### 3.11. Final consideration on non-rectangular MCHS

There are many constructive solutions to cool down electronic devices and to enhance thermal performance. However, a key role can also be played by nanofluids to reduce thermal resistance on contact surfaces and working temperatures. Water, but also oil, glycerin and ethylene glycol can be used as liquid phase and metal or metal oxide as solid phase, among which the most widely used is  $\text{Al}_2\text{O}_3$ , as Table 2 shows. This confirms what has been already pointed out also in the case described in the previous section 2. Table 2 summarizes also some of the most valuable experimental and numerical results. These results highlight that using  $\text{Al}_2\text{O}_3$  as solid phase, thermal performance of heat sinks is comparable to those where different nanoparticles, with higher thermal conductivity, but more expensive, are used.

Table 2. Summary table of the most important experimental and numerical results of this section

Researchers	Nanofluid	Particle size [nm]	Nu enhancement [%]	R <sub>T</sub> reduction [%]	h enhancement [%]	Method
Roberts <i>et al.</i> [61] - 2010	$\text{Al}_2\text{O}_3$ -water (1.0%vol)	N.A.	N.A.		18.00	Experimental
Fazeli <i>et al.</i> [67] - 2012	$\text{SiO}_2$ -water (5.0%vol)	33	N.A.	N.A.	9.00 – 15.00	Experimental
Ashjaee <i>et al.</i> [68]	$\text{Fe}_3\text{O}_4$ -water	N.A.	N.A.	N.A.	14.00 (without	Experimental

- 2015	(3.0%vol)				magnetic field) 38.00 (with magnetic field)	
Mital <i>et al.</i> [69] - 2012	Al <sub>2</sub> O <sub>3</sub> -water (2.38%vol)	N.A.	N.A.	2.15	N.A.	Numerical
Zhai <i>et al.</i> [70] - 2015	Al <sub>2</sub> O <sub>3</sub> -water (1.0%vol)	N.A.	N.A.	17.64	N.A.	Experimental
Mat Tokit <i>et al.</i> [71] - 2012	Al <sub>2</sub> O <sub>3</sub> -water (4.0%vol)	N.A.	11.1	N.A.	N.A.	Experimental
	CuO-water (4.0%wt)	N.A.	9.4	N.A.	N.A.	
	SiO <sub>2</sub> -water (4.0%wt)	N.A.	163.9	N.A.	N.A.	
Kuppusamy <i>et al.</i> [72] - 2014	Al <sub>2</sub> O <sub>3</sub> -water (1.0%wt)	N.A.	14.00	5.00	N.A.	Numerical
Sakanova <i>et al.</i> [75] - 2015	Diamond-water (1.0%vol)	N.A.	N.A.	8.52 – 10.86 (at low Reynolds) 24.10 (at high Reynolds)	N.A.	Numerical
Khoshvaght-Aliabadi <i>et al.</i> [76] - 2016	Al <sub>2</sub> O <sub>3</sub> -water (0.3%wt)	N.A.	15.20	N.A.	N.A.	Numerical
Kalteh <i>et al.</i> [78] - 2012	Al <sub>2</sub> O <sub>3</sub> -water (0.2%wt)	N.A.	20.00	N.A.	N.A.	Numerical
Rimbault <i>et al.</i> [79] - 2014	CuO-water (0.24%vol)	N.A.	Negligible	Negligible	Negligible	Experimental
Namburu <i>et al.</i> [81] - 2012	CuO-water (2.0%vol)	N.A.	100.00	N.A.	N.A.	Numerical
	CuO-water (10.0%vol)	N.A.	380.00	N.A.	151.00	
Azizi <i>et al.</i> [82] - 2015	Cu-water (0.3%wt)	N.A.	23.00	N.A.	N.A.	Experimental
Azizi <i>et al.</i> [83] - 2016	Cu-water (0.3%wt)	N.A.	N.A.	21.00	N.A.	Experimental
Ahammed <i>et al.</i> [84] - 2016	Al <sub>2</sub> O <sub>3</sub> -water (0.2%vol)	N.A.	23.92	N.A.	N.A.	Experimental
Khaleduzzaman <i>et al.</i> [85] - 2015	TiO <sub>2</sub> -water	N.A.	N.A.	20.00	N.A.	Experimental
Haasan <i>et al.</i> [88] - 2013	CuO-water (1.0%vol)	N.A.	40.00 – 110.00	N.A.	N.A.	Numerical
Yousefi <i>et al.</i> [98] - 2012	Al <sub>2</sub> O <sub>3</sub> -water (0.5%vol)	N.A.	N.A.	22.00	N.A.	Experimental
Wan <i>et al.</i> [103] - 2015	Cu-water (1.0%vol)	N.A.	N.A.	21.70	19.50	Experimental

The critical aspect of the examined papers is that low volume fraction of solid phase in nanofluid produces a negligible effect under the thermal performance point of view, as it has been demonstrated in [76], [78], [79], [82], [83], [84] and [98]. This is evident despite of the different geometrical arrangement or nanofluid's composition. Thus, to obtain a valuable increase in energy performance, that is worthy the use of nanofluids, it is necessary to use high concentration of nanoparticles (> 1.0%vol), increasing, at the same time, both pressure drop and overall costs.

#### 4. Pin fin heat sink

Popularity of microchannels among researchers and industry is due to their simple design and construction. In the last years microfabrication technology has allowed to build different microscale cooling systems among which pin fin heat sinks (PFHS) [90], which are a solution to enhance thermal performance of heat exchangers [91], increasing heat transfer area density and compactness

and reducing thermal resistance [92]. However, these advantages are paid with the cost of high pressure drop through pin array [28], although, by using heat transfer fluid with better thermal characteristics it is possible to balance the increase of pumping costs with enhancement of thermal performance.

Nguyen *et al.* [93] studied influence of Al<sub>2</sub>O<sub>3</sub>-water nanofluid at a volume fraction of 1.0%, 3.1% and 6.8% on thermal performance of a copper water block of 60 mm x 60 mm x 15 mm with a pin-finned thick base plate applied on a heated aluminum block (Figure 11), that simulated thermal power generated by a microprocessor varying volume fraction from 1.0% to 6.8%, temperature interface between base plate and aluminum block,  $T_{m,block}$ , from 40.9 °C to 37.3 °C and heat transfer coefficient from 595 W/m<sup>2</sup>K to 825 W/m<sup>2</sup>K. They observed that convective heat transfer coefficient was inversely proportional to particle size.

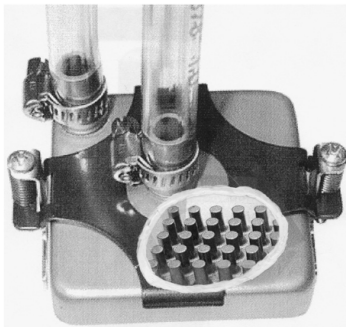


Figure 11. A view of the water-block showing its internal finned base-plate (Nguyen *et al.* [93]).

A PFHS with inline arrangement of circular pins, made of aluminum material, was tested by Duangthongsuk [94] with water, ZnO-water and SiO<sub>2</sub>-water nanofluids at volume fraction of 0.2%, 0.4% and 0.6% and heat flux from 2.0 to 5.0 W/cm<sup>2</sup>. Thermal performance of heat sink improved with nanofluids and, at the same time, Nusselt number increased with volume fraction and Reynolds number. Moreover, with ZnO-water nanofluids the best results were obtained. Actually, the values observed were 3-9% higher than those with SiO<sub>2</sub>-water nanofluids. Surface temperature of the heat sink decreased with ZnO-water and nanoparticles had no significant impact on pressure drop.

Ali *et al.* [95] investigated staggered and inline PFHSs with water, Rutile TiO<sub>2</sub> at 3.99%vol and Anatase TiO<sub>2</sub> at 4.31%vol water based nanofluids. In staggered geometry, the average of Nusselt number was 61.13% higher than that in inline geometry. Besides with Rutile-water, enhancements of average Nusselt number of 37.78% and 33.85% in staggered and inline geometry respectively were observed, compared to those obtained with water. By using Anatase-water nanofluid, enhancements were 18.30% and 16.11% respectively. Thermal resistance depended on geometry of heat sink and nanofluids. Table 3 shows reduction of thermal resistance with nanofluid, compared with water at Re=300 and it is clear that the best results were obtained with Rutile and staggered geometry.

Table 3. Reduction of thermal resistance compared with water

Nanofluid	Inline geometry	Staggered geometry
TiO <sub>2</sub> (A)-water	14.28%	28.57%
TiO <sub>2</sub> (R)-water	25.00%	35.41%

Roshani *et al.* [96] experimentally investigated a miniature plate pin finned heat sink by using Al<sub>2</sub>O<sub>3</sub>-water and TiO<sub>2</sub> water nanofluids with a volume fraction of 0.5%, 1.0%, 1.5%, and 2.0% of solid phase. A constant heat flux of 124.8 kW/m<sup>2</sup> was applied on the bottom surface of the plate PFHS. The heat sink has both length and width of 42 mm, five rectangular channels with width of 6 mm where in each of them there were 3 elliptical pin fins. Experimental results showed that temperature in the bottom side of the heat sink decreased with increasing of Reynolds number and

volume fraction. At 2.0% of  $\text{Al}_2\text{O}_3$ , temperature was lower of  $1.8^\circ\text{C}$  than that of water. With  $\text{TiO}_2$  water nanofluid, decrement was of  $1.4^\circ\text{C}$ . Convective heat transfer coefficient enhancement at 2.0% volume fraction was 16% for  $\text{Al}_2\text{O}_3$ -water and 14.0% for  $\text{TiO}_2$ -water. Decrease of thermal resistance was about 13.5% at 2.0%vol, compared with water for both nanofluids on all investigated Reynolds numbers. Increase of pumping power at high Reynolds number was about 29.0% and 32.0% for  $\text{Al}_2\text{O}_3$ -water and  $\text{TiO}_2$ -water respectively at 2.0%vol compared with water.

The same plate pin finned heat sink analyzed by Roshani, but with circular fin, was investigated by Zirakzadeh *et al.* [97]. Water and  $\text{Al}_2\text{O}_3$ -water nanofluids with volume fraction from 0.5% to 2.0% of solid phase were chosen as working fluids, coupled with a heat sink installed on the top and a heater that simulated an electronic chip with a constant heat flux of  $180 \text{ W/cm}^2$ . Experimental results showed an increase of convective heat transfer coefficient up to 16% by using nanofluids. Besides pin finned heat sink was compared with a plate fin heat sink in the same condition. In the first one convective heat transfer coefficient was 20% higher than that obtained with plate fin heat sink.

#### 4.1. Micro pin fin heat sink (MPFHS)

A micro pin fin heat sink (MPFHS) was numerically investigated under laminar flow conditions by Seyf *et al.* [98], when  $\text{CuO}$ -water and  $\text{Al}_2\text{O}_3$ -water nanofluids were used as working fluids (Figure 12).

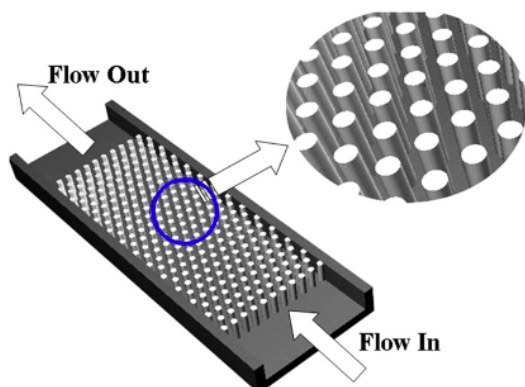


Figure 12. Schematic of the micro-pin-fin heat sink (Seyf *et al.* [98])

Average diameter of  $\text{CuO}$  particles was between 28.6 nm and 29.0 nm, whereas  $\text{Al}_2\text{O}_3$  particle size was between 38.7 nm and 47.0 nm. Nusselt number increased with Reynolds number and volume fraction. However, varying particle size, different behaviors were observed. For  $\text{Al}_2\text{O}_3$  water based nanofluid, Nusselt number was inversely proportional to particle size, whereas it was directly proportional for  $\text{CuO}$  water nanofluids. This is due to thermal conductivity of heat transfer fluid.

Hasan *et al.* [99] numerically investigated the effect of diamond-water and  $\text{Al}_2\text{O}_3$ -water nanofluids, with volume fraction between 1.0 and 4.0%, on thermal performance of an unfinned MCHS and PFHSs. The best results were obtained with Diamond-water nanofluid and with circular fins. For instance, at  $\text{Re}=900$  and volume fraction of 4.0%, enhancement of heat transfer rate of 9.12% was found for circular fins. For triangular fins and square fins, enhancement was 9.78 and 9.9% respectively. Pressure drop increased of 9.01%, 9.38% and 8.9% for square fins, triangular fins and circular fins, respectively. Pressure drop increase with  $\text{Al}_2\text{O}_3$ -water was comparable with that of diamond-water nanofluid.

Effect of  $\text{SiO}_2$ -water nanofluid on thermal performance of miniature circular fin (MCFHS) and square fin (MSFHS) was experimentally investigated by Duangthongsuk [100]. Volume fraction of solid phase was 0.2%, 0.4% and 0.6%, Reynolds number was between 700 and 3700 and heat sinks were built with aluminum. Experimental results showed that base surface temperature decreased with volume fraction and heat flux on the bottom surface of the heat sink. Enhancement of Nusselt

number between 4.0% and 14.0% was found with increasing of Reynolds number and volume fraction for both heat sink configurations. Besides, under the same condition, heat transfer coefficient with MCFHS was 6-9% higher than that obtained with MSFHS. Pressure drop increased with Reynolds number, but increase with volume fraction was negligible.

A numerical investigation with FLUENT 14 was performed to evaluate the influence of Ag-water and  $\text{Al}_2\text{O}_3$ -water nanofluids with a volume fraction of 4.0% on thermal performance of a MPFHS and an unfinned heat sink [101]. By using Ag-water nanofluid, heat transfer rate was slightly higher than  $\text{Al}_2\text{O}_3$ -water on both MPFHS and unfinned heat sink. Besides pressure drop with  $\text{Al}_2\text{O}_3$  water based nanofluid was higher than that obtained with Ag-water nanofluid. However, pressure drop into unfinned heat sink was one order of magnitude lower than that into micro pin fin heat sink. Actually, at  $\text{Re}=500$  for unfinned heat sink, pressure drop was about 25 kPa, whereas for PFHS it was about 250 kPa.

#### 4.2. Final consideration on PFHS

The use of nanofluids in PFHS increases thermal performance of the system as heat transfer coefficient or Nusselt number and decreases thermal resistance and surface temperature. Effect of nanofluids is added to that of pin fins compared to unfinned MCHS as demonstrated by some authors [99],[101]. However, in the choice of a good heat sink the increase of pressure drop or pumping power due to solid phase of nanofluids must to be taken into account.

#### 5. Heat pipes for electronic applications

Nanofluids were also employed in micro heat pipes for electronic applications. As heat pipes for solar applications, these systems are composed by evaporator, wick and condenser. Through the evaporator heat enters, vaporizing working fluid. Therefore a pressure gradient forces the vapor towards the condenser. The wick serves as a pump using capillary pressure to return the fluid from the condenser to the evaporator.

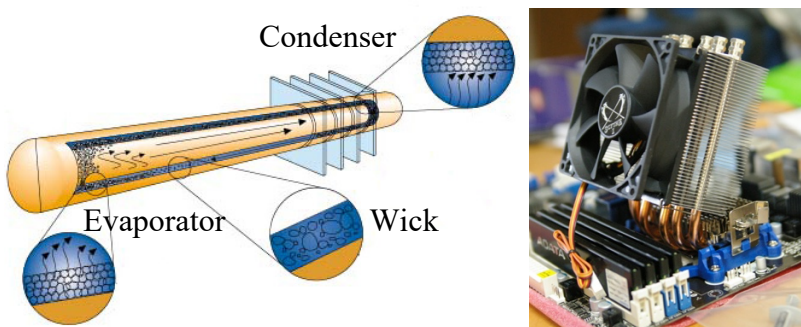


Figure 13. Example of micro heat pipe for electronic applications

Yousefi *et al.* [102] experimentally investigated a CPU cooling heat pipe taking into account the effects of inclination angle and using water and  $\text{Al}_2\text{O}_3$ -water nanofluid with weight fraction of 0.5%. CPU cooler consisted in a copper heat pipe with condensed unit attached to aluminum fin cooled by an electrical fan. Evaporator section was placed on 2 electrical heaters, that simulated CPU and GPU units respectively. From experimental results an increase of evaporator temperature for inclination angle between  $90^\circ$  and  $150^\circ$  was observed for heat flux from 5.5 W to 25 W. For instance, at 25 W the maximum value was about  $120^\circ\text{C}$ . Besides, similar behavior was found for thermal resistance that was about  $3.7^\circ\text{C}/\text{W}$  at  $90^\circ$ . By using  $\text{Al}_2\text{O}_3$ -water based nanofluid, thermal resistance decreased of 15% and 22% when heat flux was 10 W and 25 W respectively. Wan *et al.* [103] in a miniature loop heat pipe (mLHP) compared thermal performance of water and Cu-water nanofluid at a weight fraction of 1.0%, 1.5% and 2.0%. A heat transfer coefficient enhancement of 19.5% was obtained with a mass fraction of 1.0%. Besides, thermal resistance at the evaporator decreased of 21.7% with Cu-water nanofluid. Optimal mass fraction for thermal performance of

mLHP was 1.5%. Putra *et al.* [104] studied the influence of nanofluids on heat pipe liquid block, in which the evaporator zone was installed on the top of the electronic component to be cooled and the condenser zone was inserted inside a volume where coolant flowed. Water, Al<sub>2</sub>O<sub>3</sub>-water and TiO<sub>2</sub>-water nanofluids at volume fraction of 0.5% and 1.0% respectively were tested within experimental setup with inlet temperature of 25 °C, 30 °C and 35 °C and at no load and full load operating conditions of CPU. A decrease of average temperature of CPU, was observed by adding nanoparticles into water. The best results were obtained by using Al<sub>2</sub>O<sub>3</sub>-water nanofluids. With an inlet temperature of 30 °C, the average temperature of CPU using water as coolant in heat pipe liquid block, was 39.7 °C, whereas it was 38.5 °C and 37.8 °C for Al<sub>2</sub>O<sub>3</sub>-water at volume fraction of 0.5% and 1.0% respectively. By using TiO<sub>2</sub>, average temperature of CPU was 39.2 °C at 0.5%vol and 38.3 °C at 1.0 %vol. Negligible increase of pressure drop was obtained with nanofluids compared with water.

## Conclusions

Nanofluids are a very promising new generation of heat transfer fluids. In particular, the use of nanofluids in electronic devices cooling systems shows many peculiar advantages that are clear despite of the problems highlighted by many researchers.

The dispersion of both experimental and numerical results, presented in literature, demonstrates that the thermal performance of nanofluids is deeply influenced by many variables that are difficult to control. This means that thermal performance of heat sinks in general depends not only on nanofluid properties, but also on geometry.

The most used nanoparticles are Al<sub>2</sub>O<sub>3</sub>, due to their characteristics under thermo-physical and economic points of view. Actually, these nanoparticles are one of the cheapest on the market and offer good performance and stability. In all the examined works, there are no data about the problem of clogging and how to face it. It could be a big issue, particularly for high concentration (> 1.0%vol.) nanofluids, considering the narrow size of the ducts inside the heat sinks.

The thermal design of cooling systems for electronic equipment has to be revised deeply using nanofluids. It is not possible to merely substitute the traditional heat transfer fluid with a nanofluid to have an improvement of heat dissipation. All the cooling systems must be redesigned, bearing well in mind the new issues related to the peculiar characteristics of nanofluids. The researches carried out so far are not enough to have the ultimate conclusion about the real and effective advantage of using nanofluids for this application. An effort has to be done in the direction of exploring the real long-term thermal performance considering not only the advantages, but also and mainly the disadvantages (technical and mechanical problems, costs, LCA, environmental impact etc.) of this new technology.

## REFERENCES

- [1] Y. Xuan, Q. Li, *Heat transfer enhancement of nanofluids*. International Journal Heat and Fluid Flow 2000; 21: 58-64;
- [2] G. Colangelo, E. Favale, A. de Risi, D. Laforgia, *Results of experimental investigation on the heat conductivity of nanofluids based on diathermic oil for high temperature applications*. Applied Energy 2012; 97: 828-833;
- [3] H. Xie, J. Wang, T. Xi, Y. Liu, F. Ai, *Thermal conductivity enhancement of suspensions containing nanosized alumina particles*. Journal of Applied Physics 2002; 91: 4568-72;
- [4] Q. Z. Xue, *Model for effective thermal conductivity of nanofluids*. Physics Letters 2003; A307: 313-7;
- [5] C. H. Li, G. P. Peterson, *Experimental investigation of temperature and volume fraction variations on the effective thermal conductivity on nanoparticle suspensions (nanofluids)*. Journal of Applied Physics 2006; 99 (8): 084314 1-084314 8;

- [6] H. A. Minsta, G. Roy, C. T. Nguyen, D. Doucet, *New temperature dependent thermal conductivity data for water-based nanofluids*. International Journal of Thermal Sciences 2009; 48: 363-71;
- [7] W. Yu, H. Xie, L. Chen, Y. Li, *Investigation of thermal conductivity and viscosity of ethylene glycol based ZnO nanofluids*. Thermochemica Acta 2009; 491: 92-6;
- [8] J. A. Eastman, S. U. S. Choi, S. Li, W. Yu, L. J. Thompson, *Anomalous increased effective thermal conductivities of ethylene glycol-based nanofluids containing copper nanoparticles*. Applied Physics Letters 2001; 78: 718-20;
- [9] D. Wen, Y. Ding, *Experimental investigation into convective heat transfer of nanofluids at the entrance region under laminar flow conditions*. International Journal of Heat and Mass Transfer 2004; 47: 5181-88;
- [10] Rashidi F., Mosavari Nezamabad N., *Experimental investigation of convective heat transfer coefficient of CNTs nanofluid under constant heat flux*. In: Proceedings of the World Congress on Engineering 2011, vol II WCE 2011, July 6-8, London, U.K.;
- [11] K. S. Hwang, S. P. Jang, S. U. S. Choi, *Flow and convective heat transfer characteristics of water-based  $Al_2O_3$  nanofluids in fully developed laminar flow regime*. International Journal of Heat and Mass Transfer 2009; 52: 193-9;
- [12] D. Kim, Y. Kwon, Y. Cho, C. Li, S. Cheong, Y. Hwang, J. Lee, D. Hong, S. Moon, *Convective heat transfer characteristics of nanofluids under laminar and turbulent flow conditions*. Current Applied Physics 2009; 9: e119-23;
- [13] G. Colangelo, E. Favale, P. Miglietta, A. de Risi, D. Laforgia, *A new solution for reduced sedimentation flat panel solar thermal collector using nanofluids*. Applied Energy 2013; 111: 80-93;
- [14] M. M. Heyhat, F. Kowsary, A. M. Rashidi, S. Alem Varzane Esfehiani, A. Amrollahi, *Experimental investigation of turbulent flow and convective heat transfer characteristics of alumina water nanofluids in fully developed flow regime*. International Communications in Heat and Mass Transfer 2012; 39: 1272-8;
- [15] G. Colangelo, E. Favale, P. Miglietta, M. Milanese, A. de Risi, *Thermal conductivity, viscosity and stability of  $Al_2O_3$ -dithemic oil nanofluids for solar thermal energy*. Energy 2016; 95: 124-36;
- [16] S.-C. Tzeng, C.-W. Lin, K. D. Huang, C. Hua, *Heat transfer enhancement of nanofluids in rotary blade coupling of four-wheel-drive vehicles*. Acta Mechanica 2005; 179: 11-23;
- [17] M. Bai, Z. Xu, J. Lv, *Application of nanofluids in Engine cooling systems*. SAE Technical Paper 2008-01-1821;
- [18] T. Maré, S. Halelfald, O. Sow, P. Estellé, S. Duret, F. Bazantay, *Comparison of the thermal performances of two nanofluids at low temperature in a plate heat exchanger*. Experimental Thermal and Fluid Science 2011; 35: 1535-43;
- [19] B. Farajollahi, S. Gh. Etemad, M. Hojjat, *Heat transfer of nanofluids in a shell and tube heat exchanger*. International Journal of Heat and Mass Transfer 2010; 53: 12-7;
- [20] T. Yousefi, F. Veysi, E. Shojaeizadeh, S. Zinadini, *An experimental investigation on the effect of  $Al_2O_3$ - $H_2O$  nanofluid on the efficiency of flat-plate solar collectors*. Renewable Energy 2012; 39: 293-8;
- [21] T. Yousefi, F. Veysi, E. Shojaeizadeh, S. Zinadini, *An experimental investigation on the effect of MWCNT- $H_2O$  nanofluid on the efficiency of flat-plate solar collectors*. Experimental Thermal and Fluid Science 2012; 39: 207-12;
- [22] G. Colangelo, E. Favale, P. Miglietta, A. de Risi, M. Milanese, D. Laforgia, *Experimental test of an innovative high concentration nanofluid solar collector*. Applied Energy 2015; 154: 874-81;
- [23] S.M. Sohel Murshed, C.A. Nieto de Castro, *A critical review of traditional and emerging techniques and fluids for electronics cooling*, Renewable and Sustainable Energy Reviews 78 (2017) 821–833;



- [24] D. B. Tuckerman, R. F. W. Pease, *High-performance heat sinking for VLSI*. IEEE Electronics Device Letters 198; Vol. EDL-2: 126-9;
- [25] A. Mohammed Adham, N. Mohd-Ghazali, R. Ahmad, *Thermal and hydrodynamic analysis of microchannel heat sinks: A review*. Renewable and Sustainable Energy Reviews 2013; 21: 614-22;
- [26] Z. Wang, B. Sundén, Y. Li, A novel optimization framework for designing multi-stream compact heat exchangers and associated network, Applied Thermal Engineering, 2017, 116: 110-125;
- [27] Z. Wang, Y. Li, Layer pattern thermal design and optimization for multistream plate-fin heat exchangers—A review, Renewable and Sustainable Energy Reviews, 2016, 53: 500-514;
- [28] R. Remsburg, *Thermal design of electronic equipment*. New York: CRC 2001;
- [29] W. Duangthongsuk, Thermal and hydraulic performances of nanofluids flow in microchannel heat sink with multiple zigzag flow channels, MATEC Web of Conferences. EDP Sciences, 2017, 95: 03011
- [30] W. Escher, T. Brunschweiler, N. Shalkevich, A. Shalkevich, T. Burgi, B. Michel, D. Poulikakos, *On the cooling of electronics with nanofluids*. Journal of Heat Transfer 2011; 133: 051401 1-051401 10;
- [31] P. Selvakumar, S. Suresh, *Convective performance of CuO/water nanofluid in an electronic heat sink*. Experimental Thermal and Fluid Science 2012; 40: 57-63;
- [32] P. Selvakumar, S. Suresh, *Use of Al<sub>2</sub>O<sub>3</sub>-Cu/water hybrid nanofluid in an electronic heat sink*. IEEE Transaction on Components, Packaging and Manufacturing Technology 2012; 2 (10): 1600-7;
- [33] C. J. Ho, L. C. Wei, Z. W. Li, *An experimental investigation of forced convective cooling performance of a microchannel heat sink with Al<sub>2</sub>O<sub>3</sub>/water nanofluid*. Applied Thermal Engineering 2010; 30: 96-103;
- [34] C. J. Ho, W. C. Chen, *An experimental study on thermal performance of Al<sub>2</sub>O<sub>3</sub>/water nanofluid in a minichannel heat sink*. Applied Thermal Engineering 2013; 50: 516-22;
- [35] C. J. Ho, W. C. Chen, W. M. Yan, *Correlations of heat transfer effectiveness in a minichannel heat sink with water-based suspensions of Al<sub>2</sub>O<sub>3</sub> nanoparticles and/or MEPCM particles*. International Journal of Heat and Mass Transfer 2014; 69: 293-9;
- [36] P. Nitiapiruk, O. Mahian, A. S. Dalkilic, S. Wongwises, *Performance characteristics of a microchannel heat sink using TiO<sub>2</sub>/water nanofluid and different thermophysical models*. International Communications in Heat and Mass Transfer 2013; 47: 98-104;
- [37] M. R. Sohel, S. S. Khaleduzzaman, R. Saidur, A. Hepbasli, M. F. M. Sabri, I. M. Mahbubul, *An experimental investigation of heat transfer enhancement of a minichannel heat sink using Al<sub>2</sub>O<sub>3</sub>-H<sub>2</sub>O nanofluid*. International Journal of Heat and Mass Transfer 2014; 74: 164-72;
- [38] H. Zhang, A. A. O. Tay, Z. Xue, *Feasibility study of nanofluid cooling Techniques for microelectronic systems*. In: Proceedings of the 11<sup>th</sup> Electronics Packaging Technology Conference EPTC '09, December 9-11, 2009, Singapore;
- [39] S. A. Jajja, W. Ali, H. M. Ali, *Multiwalled carbon nanotube nanofluid for thermal management of high heat generating computer processor*. Heat Transfer – Asian Research 2014; 43 (7): 653-66;
- [40] S. M. Peyghambarzadeh, S. H. Hashemabadi; A. R: Chabi, M. Salimi, *Performance of water based CuO and Al<sub>2</sub>O<sub>3</sub> nanofluids in a Cu-Be alloy heat sink with rectangular microchannels*. Energy Conversion and Management 2014; 86: 28-38;
- [41] C. J. Ho, Y. N. Chung, C. M. Lai, *Thermal performance of Al<sub>2</sub>O<sub>3</sub>/water nanofluid in a natural circulation loop with a mini-channel heat sink and heat source*. Energy Conversion and Management 2014; 87: 848-58;
- [42] S. P. Jang, S. U. S. Choi, *Cooling performance of a microchannel heat sink with nanofluids*. Applied Thermal Engineering 2006; 26: 2457-63;



- [43] S. P. Jang, S. U. S. Choi, *Effect of various parameters on nanofluid thermal conductivity*. Journal of Heat Transfer 2007; 129: 617-23;
- [44] A. Ijam, R. Saidur, *Nanofluid as a coolant for electronic devices (cooling of electronic devices)*. Applied Thermal Engineering 2012; 32: 76-82;
- [45] X. L. Xie, W. Q. Tao, Y. L. He, *Numerical study of turbulent heat transfer and pressure drop characteristics in a water-cooled minichannel heat sink*. Journal of Electronic Packaging 2007; 129: 129-9;
- [46] H. A. Mohammed, P. Gunnasegaran, N. H. Shuaib, *Heat transfer in rectangular microchannels heat sink using nanofluids*. International Communications in Heat and Mass Transfer 2010; 37: 1496-1503;
- [47] C. H. Chen, C. Y. Ding, *Study on the thermal behavior and cooling performance of a nanofluid-cooled microchannel heat sink*. International Journal of Thermal Sciences 2011; 50: 378-84;
- [48] X. D. Wang, B. An, L. Lin, D. J. Lee, *Inverse geometric optimization for geometry of nanofluid-cooled microchannel heat sink*. Applied Thermal Engineering 2013; 55: 87-94;
- [49] X. D. Wang, B. An, J. L. Xu, *Optimal geometric structure for nanofluid-cooled microchannel heat sink under various constrain conditions*. Energy Conversion and Management 2013; 65: 528-38;
- [50] S. M. Hosseini Hashemi, S. A. Fazeli, H. Zirakzadeh, M. Ashjaee, *Study of heat transfer enhancement in a nanofluid-cooled miniature heat sink*. International Communications in Heat and Mass Transfer 2012; 39: 877-84;
- [51] D. Lelea, *The performance evaluation of Al<sub>2</sub>O<sub>3</sub>/water nanofluid flow and heat transfer in microchannel heat sink*. International Journal of Heat and Mass Transfer 2011; 54: 3891-9;
- [52] R. Kamali, Y. Jalali, A. R. Binesh, *Investigation of multiwalled carbon nanotube-based nanofluid advantages in microchannel heat sink*. Micro & Nano Letters 2013; 8 (6): 319-23;
- [53] R. Chein, G. Huang, *Analysis of microchannel heat sink performance using nanofluids*. Applied Thermal Engineering 2005; 25: 3104-14;
- [54] M. K. Moraveji, E. M. Ardehali, A. Ijam, *CFD investigation of nanofluid effect (cooling performance and pressure drop) in mini-channel heat sink*. International Communications in heat and Mass Transfer 2013; 40: 58-66;
- [55] T. C. Hung, W. M. Yan, W. D. Wang, C. Y. Chang, *Heat transfer enhancement in microchannel heat sink using nanofluids*. International Journal of Heat and Mass Transfer 2012; 55: 2559-70;
- [56] R. Nebbati, M. Kadja, *Study of forced convection of a nanofluid used as a heat carrier in a microchannel heat sink*. Energy Procedia 2015; 74: 633-42;
- [57] T. H. Tsai, R. Chein, *Performance analysis of nanofluid-cooled microchannel heat sink*. International Journal of Heat and Fluid Flow 2007; 28: 1013-26;
- [58] B. H. Thang, P. V. Trinh, L. D. Quang, *Heat dissipation for Intel Core i5 Processor using Multiwalled Carbon-nanotube-based Ethylene Glycol*. Journal of the Corean Physical Society 2014; 65: 312-6;
- [59] M. Korpyś, M. Al-Rashed, G. Dzido, J. Wójcik, *CPU heat sink Cooled by nanofluids and water: experimental and numerical study*. In: Proceedings of the 23<sup>rd</sup> European Symposium on Computer Aided Process Engineering – ESCAPE 23, June 9-12, 2013, Lappeenranta, Finland;
- [60] A. Turgut, E. Elbasan, *Nanofluids for electronic cooling*. In: Proceedings of the 2014 IEEE 20<sup>th</sup> International Symposium for Design and Technology in Electronic Packaging (SIITME), October 23-26, 2014, Bucharest, Romania;
- [61] N. A. Roberts, D. G. Walker, *Convective performance of nanofluids in commercial electronics cooling systems*. Applied Thermal Engineering 2010; 30: 2499-2504;
- [62] M. Rafati, A. A. Hamidi, M. Shariati Niaser, *Application of nanofluids in computer cooling systems (heat transfer performance of nanofluids)*. Applied Thermal Engineering 2012; 45-46: 9-14;

- [63] R. Chein, J. Chuang, *Experimental microchannel heat sink performance studies using nanofluids*. International Journal of Thermal Sciences 2007; 47: 57-66;
- [64] B. Fani, A. Abbassi, M. Kalteh, *Effect of nanoparticles size on thermal performance of nanofluid in a trapezoidal microchannel-heat-sink*. International Communications in Heat and Mass Transfer 2013; 45: 155-161;
- [65] H. A. Mohammed, P. Gunnasegaran, N. H. Shuaib, *Influence of various base nanofluids and substrate materials on heat transfer in trapezoidal microchannel heat sinks*. International Communication in Heat and Mass Transfer 2011; 38: 194-201;
- [66] H. A. Mohammed, P. Gunnasegaran, N. H. Shuaib, *Impact of various nanofluid types on triangular microchannels heat sink cooling performace*. International Communications in Heat and Mass Transfer 2011; 38: 767-73;
- [67] S. A. Fazeli, S. M. H. Hashemi, H. Zirakzadeh, M. Ashjaee, *Experimental and numerical investigation of heat transfer in a miniature heat sink utilizing silica nanofluid*. Superlattices and Microstructures 2012; 51: 247-64;
- [68] M. Ashjaee; M. Goharkhah, L. A. Khadem, R. Ahmadi, *Effect of magnetic field on the forced convection heat transfer and pressure drop of a magnetic nanofluid in a miniature heat sink*. Heat and Mass Transfer 2015; 51: 953-64;
- [69] M. Mital, *Evolutionary optimization of electronic circuitry cooling using nanofluid*. Model and Simulation in Engineering 2012; 2012: 8 pp, Article ID 793462
- [70] Y. I. Zhai, G. D. Xia, X. F. Liu, Y. F. Li, *Heat transfer enhancement of  $Al_2O_3-H_2O$  nanofluids flowing through a micro heat sink with complex structure*. International Communications in Heat Mass Transfer 2015; 66: 158-66;
- [71] E. Mat Tokit, H. A. Mohammed, M. Z. Yusoff, *Thermal performance of optimized interrupted microchannel heat sink (IMCHS) using nanofluids*. International Communications in Heat and Mass Transfer 2012; 39: 1595-604;
- [72] N. R. Kuppusamy, H. A. Mohammed, C. W. Lim, *Thermal and hydraulic characteristics of nanofluid in a triangular grooved microchannel heat sink (TGMCHS)*. Applied Mathematics and Computation 2014; 246: 168-83;
- [73] E. Farsad, S. P. Abbasi, M. S. Zabih; J. Sabbaghzadeh, *Numerical simulation of heat transfer in a micro channel heat sink using nanofluids*. Heat Mass Transfer 2011; 47: 479-90;
- [74] N. R. Kuppusamy, H. A. Mohammed, C. W. Lim, *Numerical investigation of trapezoidal grooved microchannel heat sink using nanofluis*. Thermochemica Acta 2013; 573: 39-56;
- [75] A. Sakanova, C. C. Keian, J. Zhao, *Performance improvements of microchannel heat sink using wavy channel and nanofluids*. International Journal of Heat and Mass Transfer 2015; 89: 59-74;
- [76] M. Khoshvaght-Aliabadi, M. Sahamiyan, *Performance of nanofluid flow in corrugated minichannels heat sink (CMCHS)*. Energy Conversion and Management 2016; 108: 197-308;
- [77] M. Izadi, M. M. Shahmardan, M. Norouzi, A. M. Rashidi, A. Behzadmehr, *Cooling performance of a nanofluid flow in a heat sink microchannel with axial conduction effect*. Applied Physics A 2014; 117: 1821-33;
- [78] M. Kalteh, A. Abbassi, M. Saffar-Avval, A. Frijns, A. Darhuber, J. Harting, *Experimental and numerical investigation of nanofluid forced convection inside a wide microchannel heat sink*. Applied Thermal Engineering 2012; 36: 260-8;
- [79] B. Rimbault, C. T. Nguyen, N. Galanis, *Experimental investigation of CuO-water nanaofluid flow and heat transfer inside a microchannel heat sink*. International Journal of Thermal Sciences 2014; 84: 275-92;
- [80] A. Radwan, M. Ahmed, S. Ookawara, *Performance enhancement of concentrated photovoltaic systems using a microchannel heat sink with nanofluids*. Energy Conversion and Management 2016; 119: 289-303;
- [81] P. K. Namburu, D. K. Das, S. R. Vajjha, *Comparison of the performance of copper oxiede nanofluid with water in electronic cooling*. Journal of ASTM International 2012; 9 No. 5, pp 15;

- [82] Z. Azizi, A. Alamdari, M. R. Malayeri, *Convective heat transfer of Cu-water nanofluid in a cylindrical microchannel heat sink*. Energy Conversion and Management 2015; 101: 515-24;
- [83] Z. Azizi, A. Alamdari, M. R. Malayeri, *Thermal performance and friction factor of a cylindrical heat sink cooled by Cu-water nanofluid*. Applied Thermal Engineering 2016; 99: 970-8;
- [84] N. Ahammed, L. G. Asirvatham, S. Wongwises, *Thermoelectric cooling of electronic devices with nanofluid in a multiport minichannel heat exchanger*. Experimental Thermal and Fluid Science 2016; 74: 81-90;
- [85] S. S. Khaleduzzaman, M. R. Sohel, R. Saidur, J. Selvaraj, *Convective performance of 0.1 % volume fraction of TiO<sub>2</sub>/water nanofluid in an electronic heat sink*. Procedia Engineering 2015; 105: 412-7;
- [86] P. Khatak, R. Jakhar, M. Kumar, *Enhancement in cooling of electronic components by nanofluids*. Journal of the Institution of Engineers (India) Serie C 2015; 96(3): 245-51;
- [87] L.-Y. Jeng, T.-P. Teng, *Performance evaluation of a hybrid cooling system for electronic chips*. Experimental Thermal and Fluid Science 2013; 45: 155-62;
- [88] N. Putra, W. N. Septiadi, R. Sahmura, C. T. Anggara, *Application of Al<sub>2</sub>O<sub>3</sub> nanofluid on sintered copper-powder vapour chamber for electronic cooling*. Advanced Materials Research 2013; 789: 423-8;
- [89] H. Hassan, *Heat transfer of Cu-water nanofluid in an enclosure with a heat sink and discrete heat source*. European Journal of Mechanics B/Fluids 2014; 45: 72-83;
- [90] H. Shaikatullah, W. R. Storr, B. J. Hansen, M. A. Gaynes, *Design and optimization of pin fin heat sink for low velocity applications*. IEEE Transaction on Components, Packaging and Manufacturing Technology – Part A 1996; 19 (4): 486-94;
- [91] D. Kim, S. J. Kim, A. Ortega, *Compact modeling of fluid flow and heat transfer in pin fin heat sink*. Journal of Electronic Packaging 2004; 126 (3): 342-50;
- [92] H. T. Chen, P. L. Chen, J. T. Horng, *Design optimization for pin-fin heat sink*. Journal of Electronic Packaging 2004; 127 (4): 397-406;
- [93] C. T. Nguyen, G. Roy, C. Gauthier, N. Galanis, *Heat transfer enhancement using Al<sub>2</sub>O<sub>3</sub>-water nanofluid for an electronic liquid cooling system*. Applied Thermal Engineering 2007; 27: 1501-6;
- [94] W. Duangthongsuk, S. Wongwises, *An experimental study on the thermal and hydraulic performances of nanofluids flow in a miniature circular pin fin heat sink*. Experimental Thermal and Fluid Science 2015; 66: 28-35;
- [95] H. M. Ali, W. Arshad, *Thermal performance investigation of staggered and inline pin fin heat sinks using water based rutile and anatase TiO<sub>2</sub> nanofluids*. Energy Conversion and Management 2015; 106: 793-803;
- [96] M. Roshani, S. Z. Miry, P. Hanafizadeh, M. Ashjaee, *Hydrodynamics and heat transfer characteristics of a miniature plate pin-fin heat sink utilizing Al<sub>2</sub>O<sub>3</sub>-water and TiO<sub>2</sub>-water nanofluids*. Journal of Thermal Science and Engineering Applications 2015; 7: 031007 1-031007 12;
- [97] H. Zirakzadeh, A. Mashayekh, H. N. Bidgoli, M. Ashjaee, *Experimental investigation of heat transfer in a novel heat sink by means of alumina nanofluids*. Heat Transfer Research 2012; 43 (8): 709-12;
- [98] H. R. Seyf, M. Feizbakhshi, *Computational analysis of nanofluid effects on convective heat transfer enhancement of micro-pin-fin heat sink*. International Journal of Thermal Sciences 2012; 58: 169-79;
- [99] M. I. Hasan, *Investigation of flow and heat transfer characteristics in micro pin fin heat sink with nanofluid*. Applied Thermal Engineering 2014; 63: 598-607;
- [100] W. Duangthongsuk, S. Wongwises, *A comparison of the heat transfer performance and pressure drop of nanofluid-cooled heat sinks with different miniature pin fin configurations*. Experimental Thermal and Fluid Science 2015; 69: 111-8;

- [101] K. Dwivedi, R. Kumar Malviya, R. Sinha, N. Mohan, *Fvm analysis for thermal and hydraulic behaviour of circular finned Mpfs by using Ag-H<sub>2</sub>O nanofluid*. International Journal of Engineering Research and Applications 2014; 4: 64-8;
- [102] T. Yousefi, S. A. Mousavi, B. Farahbakhsh, M. Z. Saghier, *Experimental investigation on the performance of CPU coolers: Effect of heat pipe inclination angle and use of nanofluids*. Microelectronics Reliability 2013; 53: 1954-61;
- [103] Z. Wan, J. Deng, B. li, Y. Xu, X. Wang, Y. Tang, *Thermal performance of a miniature loop heat pipe using water-copper nanofluid*. Applied Thermal Engineering 2015; 78: 712-9;
- [104] N. Putra, Yanuar, F. N. Iskandar, *Application of nanofluids to a heat pipe liquid-block and the thermoelectric cooling of electronic equipment*. Experimental Thermal and Fluid Science 2011; 35: 1274-81.